

Fully Asynchronous Policy Evaluation in Distributed Reinforcement Learning over Networks

Xingyu Sha [‡] Jiaqi Zhang [‡] Keyou You [‡] Kaiqing Zhang [†] Tamer Başar [†]

January 25, 2021

Abstract

This paper proposes a *fully asynchronous* scheme for the policy evaluation problem of distributed reinforcement learning (DisRL) over directed peer-to-peer networks. Without waiting for any other node of the network, each node can locally update its value function at any time by using (possibly delayed) information from its neighbors. This is in sharp contrast to the gossip-based scheme where a pair of nodes concurrently update. Though the fully asynchronous setting involves a difficult multi-timescale decision problem, we design a novel stochastic average gradient (SAG) based distributed algorithm and develop a push-pull augmented graph approach to prove its exact convergence at a linear rate of $\mathcal{O}(c^k)$ where $c \in (0, 1)$ and k increases by one no matter on which node updates. Finally, numerical experiments validate that our method speeds up linearly with respect to the number of nodes, and is robust to straggler nodes.

1 Introduction

Reinforcement learning (RL) aims to guide decision makers (aka agents) to learn optimal policies/strategies by interacting with the environment, which has achieved super-human performance in many tasks [20, 30]. This work considers the *distributed reinforcement learning (DisRL)* problem [7] over a directed *peer-to-peer* network, which includes two distinct RL setups depending on the role of the network node.

One is the so-called multi-agent RL (MARL) in which network nodes are the acting agents of MARL [15, 37, 47], and has proved its capability in solving the problems of e-sports [36], swarm robotics [16], traffic control [35] and resource allocation [18], etc. The other is the parallel RL where network nodes are designed to jointly solve a large-scale RL problem over decentralized datasets [11, 19]. The celebrated A3C in [19] adopts a master-worker configuration for parallel RL where a central node communicates with all the other nodes and is a special case of DisRL over networks.

In DisRL over networks, each node has access to a local dataset and only communicates with a subset of agents to learn the policy locally, either synchronously or asynchronously. In a synchronous model, all nodes communicate and update their learning variables in synchronized rounds via a global clock/counter [25, 37, 47], which may be hard to implement in large-scale systems [4], and suffer from deadlocks [2, 17]. While synchronous algorithms are easier to design and analysis, their efficiency is greatly dragged by the slow nodes.

To facilitate the implementation and improve the computational efficiency of the DisRL, we adopt the *fully asynchronous* model from [13] where every node can update at *any* time by using possibly delayed information from neighbors. Since we aim for *directed* communications, each node does not need to wait for others and is free of deadlocks. This is in sharp contrast to the random gossip-based asynchronous

[‡]X. Sha, J. Zhang and K. You are with the Department of Automation and BNRist, Tsinghua University, Beijing 100084, China. Emails: shaxy18@mails.tsinghua.edu.cn, zjq16@mails.tsinghua.edu.cn, youky@tsinghua.edu.cn.

[†]K. Zhang and T. Başar are with Department of Electrical and Computer Engineering and Coordinated Science Laboratory, University of Illinois at Urbana-Champaign, Urbana, IL 61801 USA. Emails: kzhang66@illinois.edu, basar1@illinois.edu.

methods where only a pair of nodes concurrently update via pairwise averaging per round [1, 17, 42]. Clearly, such a coordination between paired nodes may create deadlocks in practice and is vulnerable to information delays. It can also be problematic if a node is unable to respond or has only access to its local dataset [17]. In fact, the advantages of the fully asynchronous model has been well documented both empirically and theoretically for distributed optimization problems, see e.g. [2, 33, 45]. In this work, we study the fully asynchronous policy evaluation of the DisRL over directed networks.

The policy evaluation of MARL over networks is a rising topic and has been studied in [6, 8, 9, 28, 37]. As [6, 37], we adopt the primal-dual reformulation with a mean square projected Bellman error (MSPBE) objective function for policy evaluation. However, the striking difference is that they only consider the synchronous case with *undirected* networks. In fact, the information flow over a fully asynchronous network has only one direction since each node cannot expect any response from other nodes even if the physical communication network is bidirected. Thus the directed network is an inevitable issue in our fully asynchronous DisRL. Note that the extension from the undirected to directed networks is nontrivial in the distributed setting [38].

In the policy evaluation, we usually have to use the stochastic gradient (SG). While the SG descend method bears a vast body of literature in the centralized setting [5], it is not the case in the distributed setting, and how to design effective distributed learning algorithms with SGs has attracted an increasing attention [40]. For example, the distributed methods with SGs in [12, 21, 41, 43] are all restricted to undirected networks. Though it has been resolved in [27] via the SAGA method, it involves a division operator per iteration with a denominator that could be arbitrarily close to zero, leading to the numerical instability. It is also unclear how to extend the above mentioned works to the fully asynchronous model.

In this work, we integrate the push-pull strategy in [24, 39], which however only solve the gradient-based distributed optimization problems in a synchronous way, with the celebrated stochastic average gradient (SAG) method, and design a novel fully asynchronous push-pull SAG (APP-SAG) to find a saddle point of the primal-dual reformulation of the DisRL over directed networks.

Since the fully asynchronous setting involves a multi-timescale decision problem, the convergence proof of APP-SAG is challenging. To this end, we develop a push/pull augmented graph approach to prove the exact linear convergence of APP-SAG. Though the graph augmentation is proposed by [23], they only use one type of virtual nodes for each node, called the *pull* augmented digraph in this work. To describe APP-SAG with a single timescale, we further design a *push* augmented digraph. The push-pull augmentation scheme is also different from the augmented graph in [33] where multiple virtual edges are introduced for each edge of the network. From the worst-case point of view, we show that APP-SAG converges linearly at a deterministic rate of $\mathcal{O}(c^k)$ where $c \in (0, 1)$ mainly depends on the network topology, the level of asynchronism and the maximum delay lengths, and k increases by one no matter on which node updates.

In fact, the A3C in [19] is the first asynchronous parallel RL, where the asynchronicity is shown to have stabilizing advantages in the training process. In GALA [3], the central node of A3C is replaced with a group of learners over a directed network, which has been shown to outperform A3C in both data efficiency and robustness. Unfortunately, it cannot ensure convergence guarantees for policy evaluation. To the best of our knowledge, how to design a fully asynchronous distributed learning algorithm for the policy evaluation of DisRL over directed networks remains an open problem. Even for gradient-based distributed optimization, [1] show that a naive extension of synchronous gradient-push algorithm to the fully asynchronous model may diverge. Though it has been resolved in [45] via adaptive tuning stepsizes or gradient tracking technique in [33, 44], none of them can ensure an *exact* convergence with SGs.

Finally, APP-SAG is compared with PD-DistIAG [37] and FDPE [6] on a real networked MARL problem in [26]. We also illustrate its speedup property on the mountaincar problem from [31]. To summarize, the main contributions of this work at least include:

- (a) We have designed a fully asynchronous APP-SAG with an exact linear convergence for the policy evaluation of DisRL.
- (b) By inspecting the features of APP-SAG, we introduce the concepts of push/pull augmented digraphs to clarify our augmented approach.

(c) The celebrated SAG has been extended to the distributed setting over directed networks.

The rest of the paper is organized as follows. In Section 2, we introduce the formulation of DisRL. In Section 3, we propose APP-SAG with linear convergence guarantees. In Section 4, we construct the push/pull augmented digraphs to reformulate APP-SAG. In Section 5, we use the numerical results to validate the performance of APP-SAG. Some concluding remarks are included in Section 6. A formal proof is postponed to Appendix A.

Main notations used in this paper are given below. (1) $[\mathbf{x}_1, \dots, \mathbf{x}_n]$ and $[\mathbf{x}_1; \dots; \mathbf{x}_n]$ denote the horizontal and vertical stack of vectors $\mathbf{x}_1, \dots, \mathbf{x}_n$, respectively. (2) $\|\cdot\|_2$ denotes the l_2 -norm of a vector or matrix. $\|\cdot\|_F$ denotes the matrix Frobenius norm. $\|\cdot\|_D$ denotes the D -norm, i.e., $\|\mathbf{x}\|_D = (\mathbf{x}^\top D \mathbf{x})^{1/2}$ if the matrix D is semi-positive definite. (3) $[A]_{ij}$ denotes the (i, j) -th element of A . $\lambda_{\max}(A)$ and $\lambda_{\min}(A)$ denote the largest and smallest eigenvalues of A , respectively. (4) $\mathbf{1}_n$ and $\mathbf{0}_n$ denote the n -dimensional vector with all ones and all zeros, respectively. (5) A is nonnegative. Then it is a row-stochastic matrix if $A\mathbf{1} = \mathbf{1}$, and is column-stochastic if $\mathbf{1}^\top A = \mathbf{1}^\top$.

2 Problem formulation

2.1 DisRL over networks

Let $\mathcal{G} = (\mathcal{V}, \mathcal{E})$ be a directed network, where $\mathcal{V} = \{1, \dots, n\}$ is the set of network nodes and $\mathcal{E} \subseteq \mathcal{V} \times \mathcal{V}$ is the set of edges. A directed edge $(i, j) \in \mathcal{E}$ means that node i can directly send information to node j . Denote $\mathcal{N}_{in}^i = \{j | (j, i) \in \mathcal{E}\} \cup \{i\}$ and $\mathcal{N}_{out}^i = \{j | (i, j) \in \mathcal{E}\} \cup \{i\}$ as the sets of in-neighbors and out-neighbors of node i , respectively.

DisRL over a network is based on a finite discrete Markov decision process (MDP) with a tuple $(\mathcal{S}, \prod_{i=1}^n \mathcal{A}_i, \mathcal{P}, \{\mathcal{R}_i\}_{i=1}^n, \gamma, \mathcal{G})$, where \mathcal{S} and \mathcal{A}_i denote the state space and the action space of node i in \mathcal{G} , respectively. $\mathcal{P}(s'|s, \mathbf{a})$ is the probability of transition from $s \in \mathcal{S}$ to $s' \in \mathcal{S}$ under an action $\mathbf{a} \in \mathcal{A} := \prod_{i=1}^n \mathcal{A}_i$. $\mathcal{R}_i = \mathcal{R}_i(s, \mathbf{a}, s')$ is the reward perceived by a single node i . $\gamma \in (0, 1)$ is the discount factor. \mathcal{G} is used to model the interactions among nodes.

A stochastic policy $\pi(\mathbf{a}|s)$ is the conditional probability of taking action \mathbf{a} given a specific state s . If we focus on a target policy π , the fixed transition probability matrix is denoted as \mathcal{P}^π , whose (s, s') -th entry is given by $[\mathcal{P}^\pi]_{s, s'} = \mathcal{P}(s'|s, \pi) = \sum_{\mathbf{a} \in \mathcal{A}} \pi(\mathbf{a}|s) \cdot \mathcal{P}(s'|s, \mathbf{a})$. Let $\mathcal{R}^\pi(s) = \frac{1}{n} \sum_{i=1}^n \mathcal{R}_i^\pi(s)$, where $\mathcal{R}_i^\pi(s) = \mathbb{E}_{\mathcal{P}, \mathbf{a} \sim \pi(\cdot|s)}[\mathcal{R}_i(s, \mathbf{a}, s')]$ is the expected reward of node i at state s if the group follows π .

2.2 Policy evaluation over networks

In this work, we solve the mean squared projected Bellman error (MSPBE) problem in both MARL and parallel RL setups with experiences over networks.

Under a given policy π , value function $V^\pi(s)$ is defined as $V^\pi(s) = \mathbb{E}[\sum_{t=0}^{\infty} \gamma^t \mathcal{R}^\pi(s(t)) | s(0) = s, \pi, \mathcal{P}]$, and we simply write its vector form as $\mathbf{V}^\pi \in \mathbb{R}^{|\mathcal{S}|}$, which satisfies the Bellman equation [31] $\mathbf{V}^\pi = \mathcal{R}^\pi + \gamma \mathcal{P}^\pi \mathbf{V}^\pi$, where \mathcal{R}^π is obtained by stacking up $\mathcal{R}^\pi(s)$. In this work, we adopt a linear approximator to evaluate policy, e.g. $V^\pi(s) \approx \phi^\top(s) \boldsymbol{\theta}$, where $\phi(s) \in \mathbb{R}^d$ is a feature vector corresponding to $s \in \mathcal{S}$. That is finding a vector $\boldsymbol{\theta} \in \mathbb{R}^d$ such that $\mathbf{V}_\theta = \mathbf{\Phi} \boldsymbol{\theta} \approx \mathbf{V}^\pi$ by minimizing MSPBE. $J(\boldsymbol{\theta}) = \frac{1}{2} \|\mathbf{\Pi}_\Phi (\mathbf{V}_\theta - \gamma \mathcal{P}^\pi \mathbf{V}_\theta - \mathcal{R}^\pi)\|_D^2 + \frac{\rho}{2} \|\boldsymbol{\theta}\|^2$, where $D = \text{diag}(\boldsymbol{\mu}^\pi(s))$ and $\boldsymbol{\mu}^\pi(s)$ is the stationary distribution of states under π , $\mathbf{\Pi}_\Phi$ is the projection onto the linear subspace $\{\mathbf{\Phi} \boldsymbol{\theta}\}$, and $\frac{\rho}{2} \|\boldsymbol{\theta}\|^2$ is the regularization term. By [32], the MSPBE loss function is equivalent to

$$J(\boldsymbol{\theta}) = \frac{1}{2} \|\mathbf{A} \boldsymbol{\theta} - \mathbf{b}\|_{\mathbf{C}^{-1}}^2 + \frac{\rho}{2} \|\boldsymbol{\theta}\|^2 \quad (1)$$

where $\mathbf{A} = \mathbb{E}_{\mu^\pi}[\phi_t(\phi_t - \gamma \phi_{t+1})^\top]$, $\mathbf{b} = \mathbb{E}_{\mu^\pi}[\mathcal{R}^\pi(s(t))]$, $\mathbf{C} = \mathbb{E}_{\mu^\pi}[\phi_t \phi_t^\top]$, and ϕ_t is the short for $\phi(s(t))$.

2.2.1 Parallel RL

Parallel RL adopts multiple nodes to learn an optimal policy π . In this case, the MDP tuple of each node i is $(\mathcal{S}_i, \mathcal{A}_i, \mathcal{P}_i, \mathcal{R}_i, \gamma)$, where $\mathcal{S}_i = \mathcal{S}, \mathcal{A}_i = \mathcal{A}, \mathcal{P}_i = \mathcal{P}$ since the MDP model is identical. The local rewards may differ even under the same distribution, e.g. $\mathbb{E}_{\mathcal{P}, \mu^\pi}[\mathcal{R}_i(\mathbf{s}, \mathbf{a}, \mathbf{s}')] = \mathbb{E}_{\mathcal{P}, \mu^\pi}[\mathcal{R}_j(\mathbf{s}, \mathbf{a}, \mathbf{s}'), \forall (\mathbf{s}, \mathbf{a}, \mathbf{s}') \in \mathcal{S} \times \mathcal{A} \times \mathcal{S}, \forall i, j \in \mathcal{V}$.

Each node collects a finite sequence of samples $\mathcal{X}_i = \{\mathbf{s}_{i,p}, \mathbf{a}_{i,p}, \mathcal{R}_i(\mathbf{s}_{i,p}, \mathbf{a}_{i,p}, \mathbf{s}_{i,p+1})\}_{p=1}^{m_i}$ in the learning process. Let $m = \sum_{i=1}^n m_i$, and \mathbf{A} in (1) is estimated as $\widehat{\mathbf{A}} = \frac{m_i}{m} \sum_{i=1}^n \widehat{\mathbf{A}}_i$, where node i locally computes $\widehat{\mathbf{A}}_i = \frac{1}{m_i} \sum_{p=1}^{m_i} \widehat{\mathbf{A}}_{i,p}$ and $\widehat{\mathbf{A}}_{i,p} = \phi_{i,p}(\phi_{i,p} - \gamma \phi_{i,p+1})^\top$. Note that \mathbf{b} and \mathbf{C} are estimated analogously.

Under the distributed setting for (1), each node maintains a local copy $\{\boldsymbol{\theta}_i\}$, leading to a consensus-based form

$$\min_{\boldsymbol{\theta}} \frac{1}{2} \left\| \frac{m_i}{m} \sum_{i=1}^n (\widehat{\mathbf{A}}_i \boldsymbol{\theta}_i - \widehat{\mathbf{b}}_i) \right\|_{\widehat{\mathbf{C}}^{-1}}^2 + \frac{m_i}{m} \sum_{i=1}^n \frac{\rho}{2} \|\boldsymbol{\theta}_i\|^2 \quad (2)$$

subject to $\boldsymbol{\theta}_1 = \boldsymbol{\theta}_2 = \dots = \boldsymbol{\theta}_n$.

2.2.2 Collaborative MARL

In MARL, the nodes are heterogeneous agents over networks [46]. Each agent observes a global state \mathbf{s} and chooses an action $\mathbf{a}_i \in \mathcal{A}_i$ under its local policy $\pi_i(\mathbf{a}_i|\mathbf{s})$. The joint action $\mathbf{a} = (\mathbf{a}_1, \dots, \mathbf{a}_n)$ is then executed by the group. Thus the state transition depends on the joint policy $\boldsymbol{\pi} = (\pi_1, \dots, \pi_n)$.

Under $\boldsymbol{\pi}$, the distributed agents together collect a joint trajectory $\{\mathbf{s}_p, \mathbf{a}_p\}_{p=1}^{m_i}$, where $m_i = m_j, \forall i, j \in \mathcal{V}$, but with different reward sequences $\{\mathcal{R}_i(\mathbf{s}_p, \mathbf{a}_p, \mathbf{s}_{p+1})\}_{p=1}^{m_i}$. The agents aim to collaboratively maximize the group mean reward $\mathcal{R}(\mathbf{s}_p, \mathbf{a}_p, \mathbf{s}_{p+1}) = \frac{1}{n} \sum_{i=1}^n \mathcal{R}_i(\mathbf{s}_p, \mathbf{a}_p, \mathbf{s}_{p+1})$. The local data of i is $\mathcal{X}_i = \{\mathbf{s}_p, \mathbf{a}_p, \mathcal{R}_i(\mathbf{s}_p, \mathbf{a}_p, \mathbf{s}_{p+1})\}_{p=1}^{m_i}$. Then, the empirical MSPBE of MARL is identical to (2), except the minor difference that $m_i = m/n, \widehat{\mathbf{C}}_i = \widehat{\mathbf{C}}$ and $\widehat{\mathbf{A}}_i = \widehat{\mathbf{A}}$ for all $i \in \mathcal{V}$. In this case, \mathcal{X}_i are different though the sample sizes are identical.

2.3 MSPBE saddle-point reformulation

As in [6, 37], we adopt the conjugate form of the original \mathbf{C}^{-1} -norm, i.e.,

$$\frac{1}{2} \|\mathbf{A}\boldsymbol{\theta} - \mathbf{b}\|_{\mathbf{C}^{-1}}^2 = \max_{\boldsymbol{\omega}} (\boldsymbol{\omega}^\top (\mathbf{A}\boldsymbol{\theta} - \mathbf{b}) - \frac{1}{2} \boldsymbol{\omega}^\top \mathbf{C} \boldsymbol{\omega}),$$

and rewrite (2) as

$$\min_{\boldsymbol{\theta}_i} \max_{\boldsymbol{\omega}_i} J(\boldsymbol{\theta}_i, \boldsymbol{\omega}_i) = \frac{1}{m} \sum_{i=1}^n \sum_{p=1}^{m_i} J_{i,p}(\boldsymbol{\theta}_i, \boldsymbol{\omega}_i) \quad (3)$$

subject to $\boldsymbol{\theta}_1 = \dots = \boldsymbol{\theta}_n, \boldsymbol{\omega}_1 = \dots = \boldsymbol{\omega}_n$

where $J_{i,p}(\boldsymbol{\theta}_i, \boldsymbol{\omega}_i) = \boldsymbol{\omega}_i^\top (\widehat{\mathbf{A}}_{i,p} \boldsymbol{\theta}_i - \widehat{\mathbf{b}}_{i,p}) - \frac{1}{2} \boldsymbol{\omega}_i^\top \widehat{\mathbf{C}}_{i,p} \boldsymbol{\omega}_i + \frac{\rho}{2} \|\boldsymbol{\theta}_i\|^2$.

Clearly, $\nabla_{\boldsymbol{\theta}_i} J_{i,p}(\boldsymbol{\theta}_i, \boldsymbol{\omega}_i) = \widehat{\mathbf{A}}_{i,p}^\top \boldsymbol{\omega}_i + \rho \boldsymbol{\theta}_i$, $\nabla_{\boldsymbol{\omega}_i} J_{i,p}(\boldsymbol{\theta}_i, \boldsymbol{\omega}_i) = \widehat{\mathbf{A}}_{i,p} \boldsymbol{\theta}_i - \widehat{\mathbf{C}}_{i,p} \boldsymbol{\omega}_i - \widehat{\mathbf{b}}_{i,p}$. Throughout the paper, let $\mathbf{z}_i = [\boldsymbol{\theta}_i; \boldsymbol{\omega}_i]$, $\mathcal{M}_i = \{1, \dots, m_i\}$, and $\nabla J_{i,p_i}(\mathbf{z}_i) = [\nabla_{\boldsymbol{\theta}_i} J_{i,p_i}(\boldsymbol{\theta}_i, \boldsymbol{\omega}_i); -\nabla_{\boldsymbol{\omega}_i} J_{i,p_i}(\boldsymbol{\theta}_i, \boldsymbol{\omega}_i)]$.

3 The APP-SAG and linear convergence

3.1 The APP-SAG

In this subsection, we propose a fully asynchronous push-pull stochastic average gradient (APP-SAG) algorithm to solve (3). See Algorithm 1 for details. Note that the push-pull strategy is introduced in [24, 39] to solve the gradient-based distributed optimization problems in a synchronous way.

Algorithm 1 The APP-SAG – from the view point of node i

Initialize Set arbitrary \mathbf{z}_i , and let $\hat{\mathbf{g}}_{i,p} \leftarrow \nabla J_{i,p}(\mathbf{z}_i)$ for all $p \in \mathcal{M}_i$.

1: Compute a scaled SAG $\mathbf{y}_i \leftarrow \frac{1}{m} \sum_{p=1}^{m_i} \nabla J_{i,p_i}(\mathbf{z}_i)$ and create local buffers $\mathcal{Z}_i, \mathcal{Y}_i$.

2: Let $\tilde{\mathbf{z}}_i \leftarrow \mathbf{z}_i$, $\tilde{\mathbf{y}}_i \leftarrow \mathbf{y}_i/|\mathcal{N}_{out}^i|$, and broadcast $\tilde{\mathbf{z}}_i$ and $\tilde{\mathbf{y}}_i$ to all out-neighbors.

3: **Repeat**

4: Keep receiving $\tilde{\mathbf{z}}_j, \tilde{\mathbf{y}}_j$ from in-neighbors and save to \mathcal{Z}_i and \mathcal{Y}_i , respectively, until being activated for a new update.

5: Query the local buffers to compute

$$\mathbf{z}_i \leftarrow \text{avg}(\mathcal{Z}_i), \mathbf{y}_i \leftarrow \text{sum}(\mathcal{Y}_i), \quad (4)$$

where $\text{avg}(\cdot)$ and $\text{sum}(\cdot)$ return the average and sum over their arguments respectively.

6: Randomly pick a sample indexed by $p_i \in \mathcal{M}_i$ from the local sample set \mathcal{X}_i and update as

$$\mathbf{g}_i \leftarrow \nabla J_{i,p_i}(\mathbf{z}_i), \quad (5)$$

$$\mathbf{y}_i \leftarrow \mathbf{y}_i + \frac{1}{m} \mathbf{g}_i - \frac{1}{m} \hat{\mathbf{g}}_{i,p_i}, \quad (6)$$

$$\hat{\mathbf{g}}_{i,p_i} \leftarrow \mathbf{g}_i, \quad (7)$$

7: Update the messages to send

$$\tilde{\mathbf{z}}_i \leftarrow \mathbf{z}_i - \begin{bmatrix} \eta_1 \mathbf{I}_d & \mathbf{0} \\ \mathbf{0} & \eta_2 \mathbf{I}_d \end{bmatrix} \mathbf{y}_i, \tilde{\mathbf{y}}_i \leftarrow \mathbf{y}_i/|\mathcal{N}_{out}^i|, \quad (8)$$

where $\eta_1, \eta_2 > 0$ are two positive stepsizes.

8: Broadcast $\tilde{\mathbf{z}}_i$ and $\tilde{\mathbf{y}}_i$ to all out-neighbors, and empty \mathcal{Z}_i and \mathcal{Y}_i .

9: **Until** a stopping criteria is satisfied, e.g. $\|\mathbf{y}_i\| < \epsilon$ for a predefined $\epsilon > 0$.

We first explain how to implement Algorithm 1 in a fully asynchronous way over a directed network. Every node keeps receiving $\tilde{\mathbf{z}}_j$ and $\tilde{\mathbf{y}}_j$ from its in-neighbors and respectively copying them to its local buffers \mathcal{Z}_i and \mathcal{Y}_i , both of which may contain multiple receptions from a single in-neighbor. If node i starts to update at *any* time, it randomly picks a sample¹ from its local sample set \mathcal{X}_i and queries its buffers to perform (4)-(8). Then, it broadcasts the updated vectors $\tilde{\mathbf{z}}_i$ and $\tilde{\mathbf{y}}_i$ to all out-neighbors, which may also be subject to unpredictable but bounded delays, and empties both buffers. Clearly, there is no synchronization between nodes and is fully asynchronous, which is in sharp contrast with the gossip-based model [1, 17, 42] as the latter involves a pair of neighbors to concurrently update.

Now, we explain the key idea of APP-SAG. Inspired by our previous work [44], we use local buffers to handle asynchronicity issues and the *push-pull step* in (4) for directed networks, respectively. However, [44] does not involve any dual problem in (3) and the SG issues. As also noticed by [40], the use of SGs is non-trivial in the distributed setting and is more involved than that in the centralized setting. Particularly, a direct use of SG in distributed gradient methods cannot ensure exact convergence [40].

Thus, we extend the centralized SAG [29] to the fully asynchronous distributed setting over directed networks. Specifically, consider using the SAG method to solve a finite sample average problem, i.e.,

$$\min_{\mathbf{x} \in \mathbb{R}^d} f(\mathbf{x}) = \frac{1}{m} \sum_{p=1}^m f_p(\mathbf{x}).$$

¹It also allows to use a random mini-batch where the SAG can be obtained via the mini-batch size.

Then, the SAG at the k -th iteration is $\mathbf{h}^k = \frac{1}{m} \sum_{p=1}^m \hat{\mathbf{g}}_p^k$ where $\hat{\mathbf{g}}_p^k$ is updated as

$$\begin{cases} \hat{\mathbf{g}}_p^k \leftarrow \nabla f_p(\mathbf{x}^k), & \text{if } p = p^k, \\ \hat{\mathbf{g}}_p^k \leftarrow \hat{\mathbf{g}}_p^{k-1}, & \text{if } p \neq p^k, \end{cases}$$

and p^k is randomly chosen from sample set. That is, the SAG is iteratively updated as

$$\mathbf{h}^k \leftarrow \mathbf{h}^{k-1} + \frac{1}{m} \left(\nabla f_{p^k}(\mathbf{x}^k) - \hat{\mathbf{g}}_{p^k}^{k-1} \right). \quad (9)$$

In comparison, \mathbf{y}_i in Algorithm 1 aims to distributedly track the scaled SAG of (3) in a fully asynchronous way. Jointly with (8), our distributed algorithm then resembles the centralized SAG, which enjoys the exact linear convergence. Though more technical, one can follow a similar idea in [44] to show that \mathbf{y}_i is able to asymptotically reach consensus on a scaled value of $\bar{\mathbf{y}} = \sum_{i=1}^n \mathbf{y}_i$. Thus, we only need to check that $\bar{\mathbf{y}}$ is in fact the SAG of (3). This can be done via mathematical induction arguments. Notice from the initialization of Algorithm 1, that $\bar{\mathbf{y}} \leftarrow \frac{1}{m} \sum_{i=1}^n \sum_{p=1}^{m_i} \nabla J_{i,p}(\mathbf{z}_i)$. Now, suppose that $\bar{\mathbf{y}}$ is already an SAG. If some node i has completed a new update in Algorithm 1 and there is no transmission delay between nodes, it follows from (4)-(7) and the definition of $\tilde{\mathbf{y}}_i$ that

$$\bar{\mathbf{y}} \leftarrow \bar{\mathbf{y}} - \mathbf{y}_i + \sum_{j \in \mathcal{N}_{out}^i} \tilde{\mathbf{y}}_i = \bar{\mathbf{y}} + \frac{1}{m} (J_{i,p_i}(\mathbf{z}_i) - \hat{\mathbf{g}}_{i,p_i}) \quad (10)$$

where $\hat{\mathbf{g}}_{i,p_i}$ is given in (6) and is the latest SG before this update. In view of (9), it is clear that $\bar{\mathbf{y}}$ is indeed the SAG of (3).

Note that the local buffers are only used to illustrate the key ideas, and can be removed in practice as (4) can be recursively computed. The use of SAG requires each node to store m_i SGs, to compute only one SGs per iteration.

3.2 Linear convergence

Under the following assumptions, our main theoretical result rigorously quantifies the linear convergence of Algorithm 1.

Assumption 1. (a) *The digraph \mathcal{G} is strongly connected, i.e., any pair of nodes can be connected via a sequence of consecutive directed edges.*

(b) *Let $\mathcal{T} = \{t^k\}_{k \geq 1}$ be an increasing sequence to record the updating time instants of all nodes, e.g., $t^k \in \mathcal{T}$ if and only if one node² starts a new update at time instant t^k . There exists a constant $b > 0$ such that every node i at least completes a new update, which is also received by each of its out-neighbors, in the time interval $[t^k, t^{k+b})$ for all $t^k \in \mathcal{T}$.*

Assumption 2. (a) *The sample size is sufficiently large such that $\hat{\mathbf{A}}$ is full-rank and $\hat{\mathbf{C}}$ is positive-definite.*

(b) *Each sample in the local sample set \mathcal{X}_i is selected at least once in every K iterations.*

Assumption 1(a) is necessary, since otherwise there exist some nodes unable to be accessed by other nodes. Assumption 1(b) is easy to satisfy in practice if the communication delays are bounded and each node only takes finite time to complete one update. If the time interval between two consecutive updates is infinite for some node, it implies that such a node cannot participate in the learning process. It should be noted that the implementation of Algorithm 1 does not depend on the parameter b . Assumption 2(a) ensures the existence of a unique optimal solution for (3). Assumption 2(b) is also simple and can be easily satisfied with a random reshuffle rule [14].

Let the optimal solution of (3) be \mathbf{z}^* and denote the latest value of \mathbf{z}_i before t^k in node i by \mathbf{z}_i^k . Our main theoretical result is given below.

²If more than one node start their updates exactly at the same moment, we can simply regard them as updating successively, which will not violate our analysis in section 4.

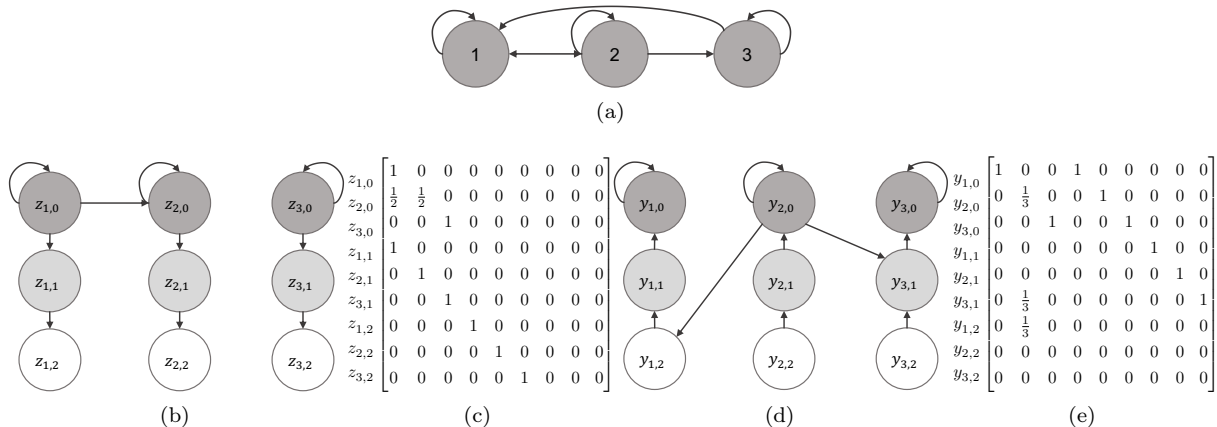


Figure 1: Consider an example with $n = 3, b = 2$ with the original graph in (a). Suppose at t^k , the activated node 2 uses \mathbf{z}_2^{k-1} from itself and \mathbf{z}_1^{k-1} from node 1's latest update to compute and send out \mathbf{z}_2^k and \mathbf{y}_2^k , which are later used by node 3 and 1 at t^{k+2} and t^{k+3} , respectively. (b) and (d) illustrate $(\mathcal{V}_z, \mathcal{E}_z^k)$ and $(\mathcal{V}_y, \mathcal{E}_y^k)$ at time t^k . (c) and (e) provide the corresponding \mathbf{H}_R^k and \mathbf{H}_C^k . Clearly, \mathbf{H}_R^k and \mathbf{H}_C^k are row- and column-stochastic matrices, respectively.

Theorem 1. Let $\eta = \eta_1, \zeta = \eta_2/\eta_1$. Suppose that Assumptions 1-2 hold and

$$\eta \in \left(0, \frac{\alpha\kappa^4(1-\kappa)^2}{72\beta^3n^3b^6K^3\tilde{t}^2}\right), \quad \zeta > \frac{4\rho + 4\lambda_{\max}(\widehat{\mathbf{A}}^\top \widehat{\mathbf{C}}^{-1} \widehat{\mathbf{A}})}{\lambda_{\min}(\widehat{\mathbf{C}}^{-1})}.$$

Then, $\|\mathbf{z}_i^k - \mathbf{z}^*\|$ converges to zero at a linear rate $\mathcal{O}(c^k)$, where $c = \max \left\{ \sqrt[2]{\frac{1}{2} + \kappa^{-1}\mu n}, \sqrt[2]{1 - \eta\alpha\kappa n/2} \right\}$, and k is increased by one no matter on which node has completed an update. The positive constants $\alpha, \beta, \kappa, \tilde{t}, \mu$ are given in Appendix A.1, and $\kappa^{-1}\mu n < 1/2$ by Corollary 1.

Remark 1. It should be noted that $\eta_2 = \eta\zeta \in \left(0, \frac{2m\beta}{\psi}\eta\right)$, where $\psi = \lambda_{\max}(\widehat{\mathbf{C}})$. See Lemma 2 in Appendix A.1 for details.

We emphasize that the deterministic convergence rate in Theorem 1 is established from the worst-case point of view, which is quite different from the random gossip scheme [1, 17, 42]. More importantly, k is unknown to any node. In synchronous algorithms, k is known to each node and is increased only if all nodes have completed their new updates, which largely confirms the computational efficiency of APP-SAG.

The proof of Theorem 1 is quite lengthy and its details are postponed to Appendix A. In Section 4, we develop an augmented system approach to provide some key results to the proof.

4 The push-pull augmented graph approach

In this section, we develop a push-pull augmented graph approach to interpret Algorithm 1 via a single timescale, which is essential to the proof of Theorem 1 in Appendix. The graph augmentation is firstly adopt in [23] for consensus problems and then extended for distributed optimization problems in [1, 45]. However, they only use one type of virtual nodes for each node of \mathcal{G} , which is called the *pull* augmented digraph in this work. Also different from [33] with augmented edges, we further design a *push* augmented digraph. Under such a push-pull augmented scheme, the push digraph aims to address \mathbf{z}_i while pull digraph is to address \mathbf{y}_i in Algorithm 1.

4.1 The push/pull augmented digraphs

For each node i of \mathcal{G} , we reindex it as $z_{i,0}$ and introduce b virtual nodes $z_{i,u}$, $u = 1, \dots, b$, where b is given in Assumption 1(b). If node i starts to update at time $t^k \in \mathcal{T}$, we construct a *pull* augmented digraph $\mathcal{G}_z^k = (\mathcal{V}_z, \mathcal{E}_z^k)$ to address the asynchronicity and delays of \mathbf{z}_i in the proof, where $\mathcal{V}_z = \{z_{i,u} | 1 \leq i \leq n, 0 \leq u \leq b\}$ and \mathcal{E}_z^k includes all the directed edges $(z_{i,u}, z_{i,u+1})$ for $0 \leq u \leq b-1$. In such an update, if node i uses \mathbf{z}_j^{k-u} from node $j \in \mathcal{N}_{in}^i$, then $(z_{j,u-1}, z_{i,0}) \in \mathcal{E}_z^k$. Note that $u \leq b-1$, and node i may use multiple receptions from node j , which implies that more than one nodes in $\{z_{j,u} | 0 \leq u \leq b\}$ are directly linked to $z_{i,0}$. Moreover, each node of \mathcal{G}_z^k pulls information from its in-neighbors and uses their *average* to update its state, which follows from the average operator in (4).

To address \mathbf{y}_i in Algorithm 1, we further construct a push augmented digraph $\mathcal{G}_y^k = (\mathcal{V}_y, \mathcal{E}_y^k)$ where the striking difference from \mathcal{G}_z^k lies in the information direction. Particularly, \mathcal{E}_y^k includes all the directed edges $(y_{i,u+1}, y_{i,u})$ for $0 \leq u \leq b-1$ and if node i uses \mathbf{y}_j^{k-u} from node $j \in \mathcal{N}_{in}^i$ at $t^k \in \mathcal{T}$, then $(y_{j,0}, y_{i,u-1}) \in \mathcal{E}_y^k$. To the contrary of the pull digraph, each node of \mathcal{G}_y^k pushes its latest state to its out-neighbors that are defined over \mathcal{E}_y^k and uses its in-neighbors' *sum* to update its state, see the summation operator in (4).

4.2 Reformulation of Algorithm 1 via a single timescale

With the aid of the push/pull digraphs, we are able to rewrite Algorithm 1 via a single timescale. To this end, let $\mathbf{z}_{i,u}^k, \mathbf{y}_{i,u}^k$, $1 \leq i \leq n, 0 \leq u \leq b$ denote the latest state of nodes $z_{i,u}, y_{i,u}$ before t^{k+1} . Let \mathcal{T}_i be an increasing sequence to record update time instants of node i . Though it is tedious, one can follow our previous [45] to show that there exist a row-stochastic matrix \mathbf{H}_R^k and a column-stochastic matrix \mathbf{H}_C^k such that Algorithm 1 is given by

$$\mathbf{Z}^{k+1} = \mathbf{H}_R^k(\mathbf{Z}^k - \eta \mathbf{I}_a^k \mathbf{Y}^k), \quad (11)$$

$$\mathbf{Y}^{k+1} = \mathbf{H}_C^k \mathbf{Y}^k + \partial^{k+1} - \partial^k, \quad (12)$$

where

$$\begin{aligned} \mathbf{Z}^k &= [\mathbf{Z}_0^k; \dots; \mathbf{Z}_n^k] \in \mathbb{R}^{\tilde{n} \times 2d}, & \mathbf{Z}_u^k &= [\mathbf{z}_{1,u}^k; \dots; \mathbf{z}_{n,u}^k] \Lambda^{-1} \in \mathbb{R}^{n \times 2d}, \\ \mathbf{Y}^k &= [\mathbf{Y}_0^k; \dots; \mathbf{Y}_n^k] \in \mathbb{R}^{\tilde{n} \times 2d}, & \mathbf{Y}_u^k &= [\mathbf{y}_{1,u}^k; \dots; \mathbf{y}_{n,u}^k] \Lambda \in \mathbb{R}^{n \times 2d}, \\ \partial^k &= [\partial J^k; \mathbf{0}_{bn \times 2d}] \in \mathbb{R}^{\tilde{n} \times 2d}, & \partial J^k &= [\partial J_1^k; \dots; \partial J_n^k] \Lambda \in \mathbb{R}^{n \times 2d}, \\ \Lambda &= [\mathbf{I}_d, \mathbf{0}; \mathbf{0}, \sqrt{\zeta} \mathbf{I}_d], \end{aligned} \quad (13)$$

$$[\mathbf{H}_R^k]_{ij} = \begin{cases} \frac{1}{|\mathcal{Z}_i^k|}, & \text{if } j = nu + v, i, v \in \mathcal{V}, t^{k+1} \in \mathcal{T}_i, i \text{ receives } \mathbf{z}_v^{k-u} \text{ at } t^{k+1}, \\ 1, & \text{if } i \in \mathcal{V}, t^{k+1} \notin \mathcal{T}_i, j = i, \\ 1, & \text{if } i \notin \mathcal{V} \text{ and } j = i - n, \\ 0, & \text{otherwise,} \end{cases}$$

$$[\mathbf{H}_C^k]_{ji} = \begin{cases} \frac{1}{|\mathcal{N}_{out}^i|}, & \text{if } j = nu + v, i, v \in \mathcal{V}, t^{k+1} \in \mathcal{T}_i, v \text{ receives } \mathbf{y}_i^k \text{ at } t^{k+u}, \\ 1, & \text{if } i \in \mathcal{V}, t^{k+1} \notin \mathcal{T}_i \text{ and } j = i, \\ 1, & \text{if } i \notin \mathcal{V} \text{ and } j = i - n, \\ 0, & \text{otherwise,} \end{cases}$$

where $|\mathcal{Z}_i^k|$ is the number of receptions in buffer \mathcal{Z}_i at time t^{k+1} . Moreover,

$$[\mathbf{I}_a^k]_{ij} = \begin{cases} 1, & \text{if } i = j, i \in \mathcal{V}, \text{ and } t^{k+1} \in \mathcal{T}_i, \\ 0, & \text{otherwise,} \end{cases} \quad (14)$$

and $\mathbf{Z}^0 = [\mathbf{Z}_0^0; \mathbf{0}_{2m \times bn}]$, $\mathbf{Y}^0 = [\partial J^0; \mathbf{0}_{2m \times bn}]$.

4.3 The distributed SAG understanding of Algorithm 1

The major difference from [44] lies in the novel use of the SAG. Note that their work does not consider the SG issues. Recall from (10) that the summation of \mathbf{y}_i aims to track the scaled SAG of $J(\cdot)$. Now, we confirm this finding in details.

If $t^k \in \mathcal{T}_i$ and node i has selected the sample p_i in Algorithm 1, let $\tau_{i,p_i}^k = k$, which is the latest iteration index for using the sample p_i . Accordingly, define

$$\begin{cases} \tau_{i,p}^k = k, & \text{if } t^k \in \mathcal{T}_i, \text{ and } p = p_i, \\ \tau_{i,p}^k = \tau_{i,p}^{k-1}, & \text{otherwise.} \end{cases} \quad (15)$$

and $\tau_{i,p}^0 = 0$ for all $p \in \mathcal{M}_i$. Jointly with (13), it implies that

$$\partial J_i^k = \frac{1}{m} \sum_{p=1}^{m_i} \nabla J_{i,p} \left(\mathbf{z}_i^{\tau_{i,p}^k} \right). \quad (16)$$

If $t^{k+1} \in \mathcal{T}_i$, it is clear from (14) that

$$\partial^{k+1} - \partial^k = \mathbf{I}_a^k (\partial^{k+1} - \partial^k).$$

By (15) and (16), the i -th row of $\partial^{k+1} - \partial^k$ is

$$\partial J_i^{k+1} - \partial J_i^k = \frac{1}{m} \sum_{p=1}^{m_i} (\nabla J_{i,p}(\mathbf{z}_i^{\tau_{i,p}^{k+1}}) - \nabla J_{i,p}(\mathbf{z}_i^{\tau_{i,p}^k})) = \frac{1}{m} (\nabla J_{i,p}(\mathbf{z}_i^{k+1}) - \nabla J_{i,p}(\mathbf{z}_i^{\tau_{i,p}^k})).$$

It follows from the initialization of Algorithm 1 that $\mathbf{y}_{i,0}^0 = \partial J_i^0 = \frac{1}{m} \sum_{p=1}^{m_i} \nabla J_{i,p}(\mathbf{z}_i^0)$. Left-multiplying $\mathbf{1}_n^\top$ on both sides of (12) leads to that

$$\mathbf{1}_n^\top \mathbf{Y}^k = \mathbf{1}_n^\top \partial^k = \frac{1}{m} \sum_{i=1}^n \sum_{p=1}^{m_i} \nabla J_{i,p} \left(\mathbf{z}_i^{\tau_{i,p}^k} \right). \quad (17)$$

By (13) and the construction of push/push digraphs, it follows that $\mathbf{1}_n^\top \mathbf{Y}^k = \sum_{i=1}^n \mathbf{y}_i^k$, if there is no transmission delays between nodes.

5 Numerical results

5.1 Experiment for MARL

We compare APP-SAG with PD-DistIAG [37] and FDPE [6] to solve a real networked MARL problem similar to [26], with 9 users/agents and 4 access points involving, see Fig. 2a. Each agent can communicate with access points on the corner of its square area. One agent keeps at most one information packet. At time t , agent i receives a new packet with probability $p_{1,i}$. The agent can then choose to keep it, with success probability $p_{2,i}$, or to send it to one of the available access points l . If simultaneously no other agents send to l , then the transmission will complete with probability q_l (dependent on l) and i will get a local reward of 1. Otherwise, if multiple agents send to the same access point l , all their transmissions will fail. In this experiment, we assume that the state of a single agent, $s_i \in \{0, 1\}$ (s_i is the package amount of the agent i), is observable to all the agents, and then the MDP obtains $2^9 = 512$ states.

We adopt a simple Sarsa algorithm with feature number $d = 10$ to learn a fixed policy. With the policy, we obtain trajectory experiences of states, actions and rewards of sample size $m_i = 5000$. We compare APP-SAG with PD-DistIAG and FDPE based on `OpenMPI` with nine CPU cores playing the roles of nodes. The network topology is undirected, see Fig. 2a. Note that PD-DistIAG and FDPE only work on undirected networks. The batch size is 1, and the stepsizes for primal/dual vectors of

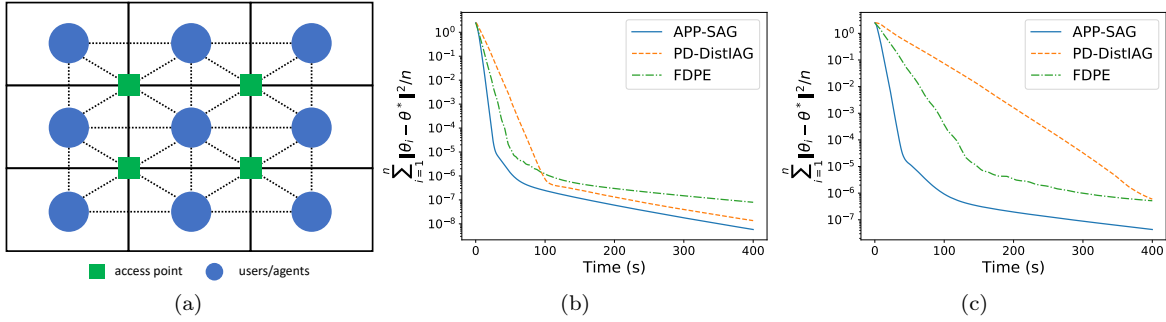


Figure 2: (a) User-access problem with nine nodes and four access points, where dot lines connect pairs of neighbors in the undirected network. (b) Convergence performance of APP-SAG, PD-DistIAG and FDPE with similar cores. (c) Convergence performance of APP-SAG, PD-DistIAG and FDPE with one core slowed down.

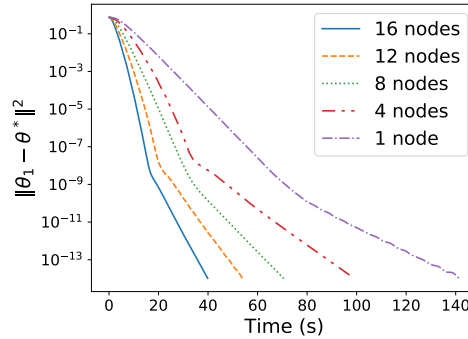


Figure 3: Speedup of APP-SAG. The speed for reaching a fixed error level increases approximately linearly with more nodes computing.

APP-SAG, PD-DistIAG and FDPE are $[\eta_1, \eta_2] = [1.4 \times 10^{-5}, 2.9 \times 10^{-4}]$, $[\eta_1, \eta_2] = [1.8 \times 10^{-5}, 8 \times 10^{-4}]$, and $[\eta_1, \eta_2] = [1.1 \times 10^{-5}, 3.8 \times 10^{-4}]$, respectively, which are manually tuned for the best performances.

In Fig. 2b, the performance of APP-SAG is consistent with our theoretical result and confirms the linear convergence to the optimal solution. Then we slow down one fixed core (the upper-right one in Fig. 2a) for both algorithms. Fig. 2c demonstrates that APP-SAG maintains its performance while PD-DistIAG and FDPE suffer greatly from the slow core.

5.2 Experiment for parallel RL

For parallel RL, we examine the speedup effect of APP-SAG, i.e., the more nodes the better convergence speed. On mountaincar task from [31], the data with feature number $d = 30$ and volume $m = 24000$, are unevenly divided to n -node networks ($n = 1, 4, 8, 12, 16$), with data volumes proportional to agent serial numbers. In the four-agent scenario, agent 1, 4 takes 1/10 and 4/10 of the total transition samples, respectively. In the network topology, each node i sends information to node $\text{mod}(2^j + i, n)$, where $0 \leq j < \lceil \log_2(n) \rceil$. The topology is directed with a connectivity of $\mathcal{O}(\log(n))$. Note that FDPE does not work in this directed network.

We set the local batch size as $64/n$, so that the problem has a fixed computational workload for networks with different numbers of nodes. The stepsizes are tuned to empirically perform best for all the node numbers, 1.1×10^{-4} , 9.6×10^{-5} , 1.3×10^{-4} , 1.5×10^{-4} , 1.9×10^{-4} for η_1 of node number 16, 12, 8, 4, 1, respectively, while $\eta_2/\eta_1 = \zeta \approx 7.0$ are similar among experiments for different node numbers. Fig. 3

shows the convergence curves of node 1 for APP-SAG under different node numbers, which verifies the APP-SAG’s linear speed-up property.

6 Conclusion

This work has proposed a novel fully asynchronous algorithm for policy evaluation of DisRL over a directed network. The striking feature allows each node to communicate with its neighbors and update its local variables locally at any time. From the worst-case view, we show that APP-SAG converges linearly with respect to a newly introduced virtual counter. Simulation results on MARL and parallel RL examples have illustrated the significance of APP-SAG. Since (3) has a specific form, our future works will consider using APP-SAG to solve general primal-dual problems.

A Proof of Theorem 1

A.1 Notations and preliminaries

Before proving Theorem 1, we provide some important properties. We first introduce an important concept called *absolute probability sequence*. [34, Theroem 4.2] claims that for any sequence of row-stochastic matrices $\{\mathbf{Q}^k\}_{k=1}^t, t \in \mathbb{N}$, there exists a sequence of stochastic vectors $\{\mathbf{u}^k\}_{k=1}^{t+1}$ that satisfies $(\mathbf{u}^{k+1})^\top \mathbf{Q}^k = (\mathbf{u}^k)^\top, \forall k \in \mathbb{N}$. Note that $\{\mathbf{u}^k\}_{k=1}^{t+1}$ depends on the whole sequence $\{\mathbf{Q}^k\}_{k=1}^t$. In (11), $\{\mathbf{H}_R^k\}$ is a row-stochastic matrices sequence and let $\{\mathbf{u}^k\}$ be the absolute probability sequence, i.e., $(\mathbf{u}^{k+1})^\top \mathbf{H}_R^k = (\mathbf{u}^k)^\top$. We use \mathbf{u}^k to track the average of \mathbf{Z}^k in the proof.

We let $\mathbf{v}^{k+1} = \mathbf{H}_C^k \mathbf{v}^k$ and $\mathbf{v}^0 = [\mathbf{1}_n; \mathbf{0}_{\tilde{n}-n}]$. Let $\mathbf{V}^k = \text{diag}(\mathbf{v}^k)$ and $(\mathbf{V}^k)^\dagger$ be the Moore-Penrose inverse of \mathbf{V}^k , i.e.,

$$[(\mathbf{V}^k)^\dagger]_{ij} = \begin{cases} 1/[\mathbf{V}^k]_{ii}, & \text{if } i = j, [\mathbf{V}^k]_{ii} > 0, \\ 0, & \text{otherwise.} \end{cases}$$

We further define

$$\mathbf{I}_V^k = \mathbf{V}^k (\mathbf{V}^k)^\dagger, \mathbf{1}_V^k = \mathbf{I}_V^k \mathbf{1}_{\tilde{n}}, \mathbf{Y}^k = (\mathbf{V}^k)^\dagger \mathbf{Y}^k, \quad (18)$$

where \mathbf{Y}^k is defined in (13). In the proof, we use \mathbf{v}^k to track the average of \mathbf{Y}^k .

In the following lemma, we show that the accumulative products of \mathbf{H}_R^k and \mathbf{H}_C^k converge to rank-one matrices linearly.

Lemma 1. ([44, Lemma 2]) Define the accumulative product of \mathbf{H}_R^k and \mathbf{H}_C^k as

$$\Phi_R^{k:k+t} = \mathbf{H}_R^{k+t-1} \dots \mathbf{H}_R^{k+1} \mathbf{H}_R^k, \quad \Phi_C^{k:k+t} = \mathbf{H}_C^{k+t-1} \dots \mathbf{H}_C^{k+1} \mathbf{H}_C^k,$$

where $k \geq 0, t > 0$. If $t = 0$, define $\Phi_R^{k:k} = \Phi_C^{k:k} = \mathbf{I}_{\tilde{n}}$.

Under Assumption 1, the following statements hold.

(a) For all $k, t \geq 0$, there exist stochastic vectors $\phi_R^{k:k+t}, \phi_C^{k:k+t} \in \mathbb{R}^{\tilde{n}}$ such that

$$\|\Phi_R^{k:k+t} - \mathbf{1}_{\tilde{n}}(\phi_R^{k:k+t})^\top\|_F \leq 2\delta^t, \quad \|\Phi_C^{k:k+t} - \phi_C^{k:k+t} \mathbf{1}_{\tilde{n}}^\top\|_F \leq 2\delta^t,$$

where $\delta = (1 - \kappa)^{1/d_g b}$ and $\kappa = (1/\tilde{n})^{d_g b} \in (0, 1)$, d_g is the diameter of \mathcal{G} , i.e., the largest distance between any pair of nodes in \mathcal{G} .

(b) For all $i \in \mathcal{V}, j \in \mathcal{V}_y, t \geq 0, \sum_{j=1}^n [\Phi_C^{0:t}]_{ij} \geq n\kappa$.

Then, Corollary 1 follows directly, by which we introduce the constant \tilde{t} and μ to characterize the long-term convergence property of our method.

Corollary 1. Under the conditions in Lemma 1, define $\tau = 2n^2(0; 1)$. There exists a constant τ_0 such that $\tau = 2$, and

$$k_R^{k;k+\tau} \mathbf{1}_R (\mathbf{k}; k+\tau)^T \mathbf{k}_F; \quad k_C^{k;k+\tau} \mathbf{1}_C (\mathbf{k}; k+\tau)^T \mathbf{k}_F; \quad 8k \geq 0. \quad (19)$$

We define $z = [z; \mathbf{1}]^T$, and

$$G_{i;p} = \frac{1}{m} \mathbf{P}^{-1} \mathbf{A}_{i;p}^T \mathbf{C}_{i;p}^{\#};$$

$$r_{j_i;p}(z) = \frac{1}{m} [r_{j_i;p}(\mathbf{1}); r_{j_i;p}(z)] = \frac{1}{m} [\mathbf{A}_{i;p}^T \mathbf{1} + \mathbf{P}^{-1} (\mathbf{A}_{i;p} \mathbf{C}_{i;p} \mathbf{1} \mathbf{b}_{i;p})];$$

$$G_i = \prod_{p=1} G_{i;p}; \quad r_{j_i}(z) = \prod_{p=1} r_{j_i;p}(z); \quad G = \prod_{i=1} G_i; \quad r_j(z) = \prod_{i=1} r_j(z);$$

We use the following lemma to study the properties of $r_j(z)$ and its corresponding gradients and SG gradients.

Lemma 2. If $\mu = \mu_1 = \mu_2$; $\mu_1 = \mu_2$ satisfies that $\mu > \frac{4 + 4 \max(\mathbf{A}^T \mathbf{C}^{-1} \mathbf{A})}{\min(\mathbf{C}^{-1})}$, and $\mu < \max(G)$, then there exists $\mu = \min(G) > 0$, such that for all $z \in \mathbb{R}^{2d}$,

$$\|z - r_j(z)\|_2 \leq (1 - \mu) \|z\|_2; \quad (20)$$

and for all $z_1, z_2 \in \mathbb{R}^{2d}$; $8i; p$;

$$\|r_{j_i;p}(z_1) - r_{j_i;p}(z_2)\|_2 \leq \|z_1 - z_2\|_2; \quad (21)$$

where $\mu = \max_{1 \leq i \leq n; 1 \leq p \leq m_i} \min(G_{i;p})$. Define $\mu = \min(\mathbf{C})$, then

$$\mu > \frac{1}{2m}; \quad (22)$$

Proof. According to [10, Appendix A], if $\mu > \frac{4 + 4 \max(\mathbf{A}^T \mathbf{C}^{-1} \mathbf{A})}{\min(\mathbf{C}^{-1})}$, G is a diagonalizable matrix with all eigenvalues of G are positive and real. By direct computation, we can verify that

$$z - r_j(z) = (I - G)(z - r_j(z));$$

where $\|I - G\|_2 \leq \frac{1}{\min(G)}$. Define $\mu = \min(G)$ and (20) follows.

By computation, for all $z_1, z_2 \in \mathbb{R}^{2d}$; $r_{j_i}(z_1) - r_{j_i}(z_2) = G_i(z_1 - z_2)$; $r_{j_i;p}(z_1) - r_{j_i;p}(z_2) = G_{i;p}(z_1 - z_2)$; and (21) follows.

Let $x \in \mathbb{R}^d$ be an arbitrary eigenvector of \mathbf{C} that $\mathbf{C}x = \mu x$. Note that

$$G = \mathbf{P}^{-1} \mathbf{A} \mathbf{C} \mathbf{P};$$

then $[x; x]^T G [x; x] = \frac{1}{m} (\mu + \mu) x^T x$. By diagonalizability, $[x; x]^T G [x; x] \leq \max(G) x^T x$, and then $\frac{1}{m} \max(G) > \frac{1}{2m} \mu$ holds for all the eigenvalues of \mathbf{C} . Thus, (22) is in force. ■

A.2 Proof Sketch of Theorem 1

We define the following quantities.

(a) $k_Z^k k_F = k_T^k Z^k k_F$, where $T_{ij}^k = \mathbf{1}_R (\mathbf{u}^k)^T$, which is the weighted consensus error $\alpha^k z^k$ in the augmented network.

- (b) $\|\check{\mathbf{Y}}_V^k\|_F = \|\mathbf{T}_C^k \mathbf{Y}_V^k\|_F$, where $\mathbf{T}_C^k = \mathbf{I}_V^k - \frac{1}{n} \mathbf{1}_V^k (\mathbf{v}^k)^\top$, which is an error estimate corresponding to the gradient surrogates.
- (c) $\|\check{\mathbf{z}}_U^k\|_F$, where $\check{\mathbf{z}}_U^k = \mathbf{z}_U^k - \mathbf{z}^* = (\mathbf{Z}^k)^\top \mathbf{u}^k - \mathbf{z}^*$, which is the optimality gap between the weighted average and the saddle point.

Then, $\check{\mathbf{Z}}^k$, $\check{\mathbf{Y}}_V^k$, $\check{\mathbf{z}}_U^k$ and \mathbf{Y}^k are bounded for all $k \geq 0$, i.e.,

$$\|\check{\mathbf{Z}}^{k+\tilde{t}}\|_F \leq 2\mu \|\check{\mathbf{Z}}^k\|_F + \eta\sqrt{2\tilde{n}} \sum_{t=0}^{\tilde{t}-1} \|\mathbf{Y}^{k+t}\|_F, \quad (23)$$

$$\|\check{\mathbf{Y}}_V^{k+\tilde{t}}\|_F \leq 2\kappa^{-1}\mu n \|\check{\mathbf{Y}}_V^k\|_F + 2\beta\kappa^{-1}\sqrt{\tilde{n}}bK \sum_{t=-bK}^{\tilde{t}-1} (2\|\check{\mathbf{Z}}^{k+t}\|_F + \eta\|\mathbf{Y}^{k+t}\|_F), \quad (24)$$

$$\begin{aligned} \|\check{\mathbf{z}}_U^{k+b}\|_F &\leq (1 - \eta\alpha bn) \|\check{\mathbf{z}}_U^k\|_F + \eta n \sum_{t=0}^{b-1} \|\check{\mathbf{Y}}_V^{k+t}\|_F + 3\eta n \beta \sum_{t=0}^{b-1} \|\check{\mathbf{Z}}^{k+t}\|_F \\ &\quad + \eta mbK\beta \sum_{t=-bK}^{b-1} (2\sqrt{n}\|\check{\mathbf{Z}}^{k+t}\|_F + \eta\|\mathbf{Y}^{k+t}\|_F), \end{aligned} \quad (25)$$

$$\|\mathbf{Y}^k\|_F \leq n\|\check{\mathbf{Y}}_V^k\|_F + 2\beta\sqrt{\tilde{n}n} \sum_{t=k-bK}^k \|\check{\mathbf{Z}}^t\|_F + \beta\sqrt{\tilde{n}n} \sum_{t=k-bK}^k \|\mathbf{z}_U^t - \mathbf{z}^*\|_F, \quad (26)$$

where \tilde{t} and μ are given in Corollary 1, κ is as introduced in Lemma 1, α, β are in Lemma 2, and b, K from Assumption 1(b), 2(b). Any value with $k < 0$ is regarded as 0. The above inequalities will be formally proved in Appendix A.3.

To prove the convergence of the inequality linear system (23)-(26), we introduce λ -sequence from [22]. Then, the proof of Lemma 3 directly follows the proof of [44, Lemma 8].

Definition 1. Let $\{\mathbf{p}^t\}$ be a nonnegative sequence with $\lambda \in (0, 1)$, the λ -sequence of \mathbf{p}^k be $\mathbf{p}^{\lambda, k} = \sup_{1 \leq t \leq k} \frac{\mathbf{p}^t}{\lambda^t}$. If $\mathbf{p}^{\lambda, k}$ is bounded by \bar{p} for all k , then $\mathbf{p}^k \leq \bar{p}\lambda^k$.

Lemma 3. Let $\{\mathbf{p}^k\}, \{\mathbf{q}^k\}$ be nonnegative sequences satisfying $\mathbf{p}^{t+j+1} \leq r\mathbf{p}^{t+1} + \sum_{i=0}^{j+1-1} \mathbf{q}^{t+i}$, where $r \in [0, 1)$ is a scalar. If we choose λ such that $\lambda^j \in (r, 1)$, then the λ -sequences $\mathbf{p}^{\lambda, k}$ and $\mathbf{q}^{\lambda, k}$ satisfy $\mathbf{p}^{\lambda, k} \leq \frac{j+1}{\lambda^j - r} \mathbf{q}^{\lambda, k} + c_\lambda$, $\forall k \in \mathbb{N}$, where $c_\lambda = \frac{\lambda^j}{\lambda^j - r} \sum_{t=1}^m \lambda^{-t} \mathbf{p}^t$ is a constant not related to k .

Based on Lemma 3 and (23)-(26), we can derive the following relationship between the λ -sequence corresponding to the above quantities. For all $k \geq 1$, if $\lambda = \max \left\{ \sqrt[\tilde{t}+1]{\frac{1}{2} + \kappa^{-1}\mu n}, \sqrt[6+1]{1 - \eta\alpha\kappa n/2} \right\}$, the following inequalities hold,

$$\begin{aligned} \|\check{\mathbf{Z}}\|_F^{\lambda, k} &\leq \frac{2\eta n^2 \sqrt{2\tilde{n}\tilde{t}}}{\kappa^2(n-1)} \|\mathbf{Y}\|_F^{\lambda, k} + p_1, \\ \|\check{\mathbf{Y}}_V\|_F^{\lambda, k} &\leq \frac{4\beta\sqrt{\tilde{n}\tilde{t}}bK}{\kappa^2(1-\kappa)} \left(2\|\check{\mathbf{Z}}\|_F^{\lambda, k} + \eta\|\mathbf{Y}\|_F^{\lambda, k} \right) + p_2, \\ \|\check{\mathbf{z}}_U\|_F^{\lambda, k} &\leq \frac{1}{(1-\eta\alpha\kappa n)\alpha\kappa} \left((6nb\beta + 8b^2K^2\beta\sqrt{n})\|\check{\mathbf{Z}}\|_F^{\lambda, k} + 2b\|\check{\mathbf{Y}}_V\|_F^{\lambda, k} + 2\eta b^2K^2\beta\|\mathbf{Y}\|_F^{\lambda, k} \right) + p_3, \\ \|\mathbf{Y}\|_F^{\lambda, k} &\leq 2\beta\sqrt{\tilde{n}\tilde{n}}bK\|\check{\mathbf{Z}}\|_F^{\lambda, k} + n\|\check{\mathbf{Y}}_V\|_F^{\lambda, k} + \beta\sqrt{\tilde{n}\tilde{n}}bK\|\check{\mathbf{z}}_U\|_F^{\lambda, k}, \end{aligned}$$

where p_1, p_2, p_3 are constants, and $\|\check{\mathbf{Z}}\|_F^{\lambda, k}$, $\|\check{\mathbf{Y}}_V\|_F^{\lambda, k}$, $\|\check{\mathbf{z}}_U\|_F^{\lambda, k}$, $\|\mathbf{Y}\|_F^{\lambda, k}$ are λ -sequences of $\|\check{\mathbf{Z}}^k\|_F$, $\|\check{\mathbf{Y}}_V^k\|_F$, $\|\check{\mathbf{z}}_U^k\|_F$, $\|\mathbf{Y}^k\|_F$, respectively.

Let $\mathbf{d}^{\lambda,k} = [\|\check{\mathbf{Z}}\|_{\mathbb{F}}^{\lambda,k}; \|\check{\mathbf{Y}}_{\mathbf{V}}\|_{\mathbb{F}}^{\lambda,k}; \|\check{\mathbf{z}}_{\mathbf{U}}\|_{\mathbb{F}}^{\lambda,k}; \|\mathbf{Y}\|_{\mathbb{F}}^{\lambda,k}]$, then $\mathbf{d}^{\lambda,k} \preceq \mathbf{Q}\mathbf{d}^{\lambda,k} + \mathbf{p}$, and

$$\mathbf{Q} = \begin{bmatrix} 0 & 0 & 0 & \frac{2\eta n^2 \sqrt{2\tilde{n}t}}{\kappa^2(n-1)} \\ \frac{8\beta\sqrt{\tilde{n}tb}K}{\kappa^2(1-\kappa)} & 0 & 0 & \frac{4\eta\beta\sqrt{\tilde{n}tb}K}{\kappa^2(1-\kappa)} \\ \frac{6bn\beta+8b^2K^2\beta\sqrt{\tilde{n}}}{(1-\eta\alpha\kappa n)\alpha\kappa} & \frac{2b}{(1-\eta\alpha\kappa n)\alpha\kappa} & 0 & \frac{2\eta b^2K^2\beta}{(1-\eta\alpha\kappa n)\alpha\kappa} \\ 2\beta\sqrt{n\tilde{n}b}K & n & \beta\sqrt{n\tilde{n}b}K & 0 \end{bmatrix}.$$

Clearly, $\|\mathbf{Q}\| < 1$ if η is sufficiently small. Then, $\mathbf{d}^{\lambda,k}$ is bounded and $\|\check{\mathbf{Z}}^k\|_{\mathbb{F}}, \|\check{\mathbf{z}}_{\mathbf{U}}^k\|_{\mathbb{F}}$ converges to 0 at the rate of $\mathcal{O}(\lambda)$. Moreover,

$$\|\mathbf{z}_i^k - \mathbf{z}^*\|_{\mathbb{F}} \leq 2\|\check{\mathbf{Z}}^k\|_{\mathbb{F}} + \|\check{\mathbf{z}}_{\mathbf{U}}^k\|_{\mathbb{F}}, \forall i \in \mathcal{V}, \forall k,$$

which leads to the result in the Theorem 1.

An upper bound of η can be given by bounding $\|\mathbf{Q}^4\|_{\infty}$ to ensure that the spectral radius of \mathbf{Q} is strictly less than 1. The bound is as described in Theorem 1, i.e., $\eta \in \left(0, \frac{\alpha\kappa^4(1-\kappa)^2}{72\beta^3n^3b^6K^3t^2}\right)$. Noticing (22) from Lemma 2, we further obtain the bound for $\eta_2 = \eta\zeta$ in Remark 1.

A.3 Proofs of (23)-(26)

A.3.1 Proof of (23)

Recalling the definition of $\check{\mathbf{Z}}^k$ in Appendix A.2, it follows from (11), we have

$$\|\check{\mathbf{Z}}^{k+\tilde{t}}\|_{\mathbb{F}} = \|\mathbf{T}_{\mathbf{U}}^{k+\tilde{t}}\mathbf{Z}^{k+\tilde{t}}\|_{\mathbb{F}} \leq \|\mathbf{T}_{\mathbf{U}}^{k+\tilde{t}}\phi_{\mathbf{R}}^{k:k+\tilde{t}}\mathbf{Z}^k\|_{\mathbb{F}} + \eta \sum_{t=0}^{\tilde{t}-1} \|\mathbf{T}_{\mathbf{U}}^{k+\tilde{t}}\phi_{\mathbf{R}}^{k:k+\tilde{t}}\mathbf{I}_a^{k+t}\mathbf{Y}^{k+t}\|_{\mathbb{F}}. \quad (27)$$

For the first term in (27), we use the property that \mathbf{u}^k is row-stochastic and obtain

$$\begin{aligned} \mathbf{T}_{\mathbf{U}}^{k+\tilde{t}}\phi_{\mathbf{R}}^{k:k+\tilde{t}} &= (\mathbf{I}_{\tilde{n}} - \mathbf{1}_{\tilde{n}}(\mathbf{u}^{k+\tilde{t}-1})^{\top})\phi_{\mathbf{R}}^{k:k+\tilde{t}} \\ &= (\mathbf{I}_{\tilde{n}} - \mathbf{1}_{\tilde{n}}(\mathbf{u}^{k+\tilde{t}-1})^{\top})(\phi_{\mathbf{R}}^{k:k+\tilde{t}} - \mathbf{1}_{\tilde{n}}(\mathbf{u}^{k-1})^{\top}) - (\mathbf{I}_{\tilde{n}} - \mathbf{1}_{\tilde{n}}(\mathbf{u}^{k+\tilde{t}-1})^{\top})(\mathbf{1}_{\tilde{n}}(\phi_{\mathbf{R}}^{k:k+\tilde{t}})^{\top} - \mathbf{1}_{\tilde{n}}(\mathbf{u}^{k-1})^{\top}) \\ &= (\mathbf{I}_{\tilde{n}} - \mathbf{1}_{\tilde{n}}(\mathbf{u}^{k+\tilde{t}-1})^{\top})(\phi_{\mathbf{R}}^{k:k+\tilde{t}} - \mathbf{1}_{\tilde{n}}(\phi_{\mathbf{R}}^{k:k+\tilde{t}})^{\top})(\mathbf{I}_{\tilde{n}} - \mathbf{1}_{\tilde{n}}(\mathbf{u}^{k-1})^{\top}) \\ &= \mathbf{T}_{\mathbf{U}}^{k+\tilde{t}}(\phi_{\mathbf{R}}^{k:k+\tilde{t}} - \mathbf{1}_{\tilde{n}}(\phi_{\mathbf{R}}^{k:k+\tilde{t}})^{\top})\mathbf{T}_{\mathbf{U}}^k, \end{aligned} \quad (28)$$

Since $\|\mathbf{AB}\|_{\mathbb{F}} \leq \|\mathbf{A}\|_2\|\mathbf{B}\|_{\mathbb{F}}$ and $\|\mathbf{AB}\|_{\mathbb{F}} \leq \|\mathbf{A}\|_{\mathbb{F}}\|\mathbf{B}\|_{\mathbb{F}}$, we obtain

$$\|\mathbf{T}_{\mathbf{U}}^{k+\tilde{t}}\phi_{\mathbf{R}}^{k:k+\tilde{t}}\mathbf{Z}^k\|_{\mathbb{F}} \leq \|\mathbf{T}_{\mathbf{U}}^{k+\tilde{t}}\|_2\|\phi_{\mathbf{R}}^{k:k+\tilde{t}} - \mathbf{1}_{\tilde{n}}\phi_{\mathbf{R}}^{k:k+\tilde{t}}\|_{\mathbb{F}}\|\mathbf{T}_{\mathbf{U}}^k\mathbf{Z}^k\|_{\mathbb{F}} \leq 2\mu\|\check{\mathbf{Z}}^k\|_{\mathbb{F}}, \quad (29)$$

where the last inequality follows from $\|\mathbf{T}_{\mathbf{U}}^{k+\tilde{t}}\|_2 = \|\mathbf{I}_{\tilde{n}} - \mathbf{1}_{\tilde{n}}(\mathbf{u}^{k+\tilde{t}-1})^{\top}\|_2 < 2$ and Corollary 1.

For the second term in (27), it holds that

$$\eta \sum_{t=0}^{\tilde{t}-1} \|\mathbf{T}_{\mathbf{U}}^{k+\tilde{t}}\phi_{\mathbf{R}}^{k:k+\tilde{t}}\mathbf{I}_a^{k+t}\mathbf{Y}^{k+t}\|_{\mathbb{F}} \leq \eta\|\mathbf{T}_{\mathbf{U}}^{k+\tilde{t}}\|_2 \sum_{t=0}^{\tilde{t}-1} \|\phi_{\mathbf{R}}^{k:k+\tilde{t}}\mathbf{I}_a^{k+t}\mathbf{Y}^{k+t}\|_{\mathbb{F}} \leq \eta\sqrt{2\tilde{n}} \sum_{t=0}^{\tilde{t}-1} \|\mathbf{Y}^{k+t}\|_{\mathbb{F}}, \quad (30)$$

where $\|\phi_{\mathbf{R}}^{k:k+\tilde{t}}\|_2 \leq \sqrt{\tilde{n}/2}, \forall t \geq 0$. The desired result then follows by combining (29) and (30).

A.3.2 Proof of (24)

To study $\mathbf{Y}_{\mathbf{V}}^k$ defined in (18), let

$$\mathbf{H}_{\mathbf{V}}^k = (\mathbf{V}^{k+1})^{\dagger}\mathbf{H}_{\mathbf{C}}^k\mathbf{V}^k. \quad (31)$$

Furthermore, we define $\Phi_{\mathbf{V}}^{k:k+t} = \prod_{j=k}^{k+t-1}\mathbf{H}_{\mathbf{V}}^j$, and demonstrate that $\Phi_{\mathbf{V}}^{k:k+t}$ converges to a rank-one matrix, i.e.,

$$\left\|\Phi_{\mathbf{V}}^{k:k+\tilde{t}} - \frac{1}{n}\mathbf{1}_{\mathbf{V}}^k(\mathbf{v}^k)^{\top}\right\|_{\mathbb{F}} < \kappa^{-1}\mu n < \frac{1}{2}. \quad (32)$$

To show (32), first,

$$\begin{aligned}
\Phi_{\mathbf{V}}^{k:k+t} &= \mathbf{H}_{\mathbf{V}}^{k+t-1} \dots \mathbf{H}_{\mathbf{V}}^k \\
&= (\mathbf{V}^{k+t})^\dagger \mathbf{H}_{\mathbf{C}}^{k+t-1} \mathbf{I}_{\mathbf{V}}^{k+t-1} \dots \mathbf{H}_{\mathbf{C}}^k \mathbf{V}^k \\
&= (\mathbf{V}^{k+t})^\dagger \Phi_{\mathbf{C}}^{k:k+t} \mathbf{V}^k.
\end{aligned}$$

The last equality is tenable because $\mathbf{I}_{\mathbf{V}}^{k+1} \mathbf{H}_{\mathbf{C}}^k \mathbf{V}^k = \mathbf{H}_{\mathbf{C}}^k \mathbf{V}^k, \forall k \geq 0$, which together with $\mathbf{v}^{k+1} = \mathbf{H}_{\mathbf{C}}^k \mathbf{v}^k$, can be verified by computing each row on both sides.

By Lemma 1(a), there exists $\Delta \Phi_{\mathbf{C}}^{k:k+t} \in \mathbb{R}^{\tilde{n} \times \tilde{n}}$ such that $\|\Delta \Phi_{\mathbf{C}}^{k:k+t}\|_{\mathbb{F}} \leq 2\delta^t$, and $\phi_{\mathbf{C}}^{k:k+t} \mathbf{1}_{\tilde{n}}^\top + \Delta \Phi_{\mathbf{C}}^{k:k+t} = \Phi_{\mathbf{C}}^{k:k+t}$. Right multiplying \mathbf{v}^k on both sides yields $\phi_{\mathbf{C}}^{k:k+t} \mathbf{1}_{\tilde{n}}^\top \mathbf{v}^k + \Delta \Phi_{\mathbf{C}}^{k:k+t} \mathbf{v}^k = \Phi_{\mathbf{C}}^{k:k+t} \mathbf{v}^k = \mathbf{v}^{k+t}$. Since $\phi_{\mathbf{C}}^{k:k+t} \mathbf{1}_{\tilde{n}}^\top \mathbf{v}^k = \phi_{\mathbf{C}}^{k:k+t} \mathbf{1}_{\tilde{n}}^\top \mathbf{v}^0 = n \phi_{\mathbf{C}}^{k:k+t}$, we have $\phi_{\mathbf{C}}^{k:k+t} = \frac{1}{n}(\mathbf{v}^{k+t} - \Delta \Phi_{\mathbf{C}}^{k:k+t} \mathbf{v}^k)$. Then,

$$\begin{aligned}
\left\| \Phi_{\mathbf{V}}^{k:k+t} - \frac{\mathbf{1}_{\mathbf{V}}^k (\mathbf{v}^k)^\top}{n} \right\|_{\mathbb{F}} &= \left\| \Phi_{\mathbf{V}}^{k:k+t} - \frac{(\mathbf{V}^{k+t})^\dagger \mathbf{v}^{k+t} \mathbf{1}_{\tilde{n}}^\top \mathbf{V}^k}{n} \right\|_{\mathbb{F}} \\
&= \left\| (\mathbf{V}^{k+t})^\dagger \Delta \Phi_{\mathbf{C}}^{k:k+t} \left(\mathbf{I}_{\tilde{n}} - \frac{\mathbf{v}^k \mathbf{1}_{\tilde{n}}^\top}{n} \right) \right\|_{\mathbb{F}} \\
&\leq \|(\mathbf{V}^{k+t})^\dagger\|_2 \|\Delta \Phi_{\mathbf{C}}^{k:k+t}\|_{\mathbb{F}} \left\| \left(\mathbf{I}_{\tilde{n}} - \frac{\mathbf{v}^k \mathbf{1}_{\tilde{n}}^\top}{n} \right) \right\|_{\mathbb{F}} \\
&< \kappa^{-1} \cdot 2\delta^t \cdot n,
\end{aligned} \tag{33}$$

where we have used the fact that all the entries of $(\mathbf{V}^k)^\dagger$ are less than κ^{-1} from Lemma 1(b). (32) follows directly by substituting \tilde{t} into (33).

Define $\mathbf{D}^k = \partial J^{k+1} - \partial J^k$ and rewrite the update (12) as

$$\mathbf{Y}_{\mathbf{V}}^{k+1} = \mathbf{H}_{\mathbf{V}}^k \mathbf{Y}_{\mathbf{V}}^k + (\mathbf{V}^{k+1})^\dagger \mathbf{D}^k. \tag{34}$$

Then, β is from Lemma 2, and \mathbf{D}^k is bounded for all $k \geq 0$ as below

$$\begin{aligned}
\|\mathbf{D}^k\|_{\mathbb{F}} &= \|\nabla j_{i,p_{k+1}}(\mathbf{z}_i^{k+1}) - \nabla j_{i,p_{k+1}}(\mathbf{z}_i^{\tau_{i,p}^k, p^{k+1}})\|_{\mathbb{F}} \\
&\leq \beta \sum_{t=\tau_{i,p}^k}^k \|\mathbf{z}_i^{t+1} - \mathbf{z}_i^t\| \\
&\leq \beta \sum_{t=k-bK}^k \|\mathbf{z}_i^{t+1} - \mathbf{z}_i^t\| \\
&\leq \beta \sum_{t=k-bK}^k \|\mathbf{I}_a^k (\mathbf{Z}^{t+1} - \mathbf{Z}^t)\|_{\mathbb{F}} \\
&\leq \beta \sum_{t=k-bK}^k (\|\mathbf{I}_a^k \mathbf{H}_{\mathbf{R}}^t - \mathbf{I}_a^k\|_{\mathbb{F}} \|\mathbf{T}_{\mathbf{U}}^t \mathbf{Z}^t\|_{\mathbb{F}} + \eta \|\mathbf{Y}^t\|_{\mathbb{F}}) \\
&\leq \beta \sum_{t=k-bK}^k (2\|\tilde{\mathbf{Z}}^t\|_{\mathbb{F}} + \eta \|\mathbf{Y}^t\|_{\mathbb{F}})
\end{aligned} \tag{35}$$

where the second inequality follows Assumption 1(b), 2(b), and the last from the row-stochasticity of $\mathbf{H}_{\mathbf{R}}^k$.

Next, we prove (24) in a similar way as in Section A.3.1. By (34), we get

$$\begin{aligned}
\|\check{\mathbf{Y}}_V^{k+\tilde{t}}\|_F &= \left\| \mathbf{T}_C^{k+\tilde{t}} \mathbf{Y}_V^{k+\tilde{t}} \right\|_F \\
&\leq \left\| \mathbf{T}_C^{k+\tilde{t}} \Phi_V^{k:k+\tilde{t}} \mathbf{Y}_V^k \right\|_F + \sum_{t=0}^{\tilde{t}-1} \left\| \left(\mathbf{I}_V^{k+\tilde{t}} - \frac{1}{n} \mathbf{1}_V^{k+\tilde{t}} (\mathbf{v}^{k+\tilde{t}})^\top \right) \Phi_V^{k+t+1:k+\tilde{t}} (\mathbf{V}^{k+t+1})^\dagger \mathbf{D}^{k+t} \right\|_F \\
&\leq 2\kappa^{-1} \mu n \|\check{\mathbf{Y}}_V^k\|_F + \sum_{t=0}^{\tilde{t}-1} 2\sqrt{\tilde{n}} \kappa^{-1} \|\mathbf{D}^{k+t}\|_F,
\end{aligned} \tag{36}$$

where the last inequality is from (32), and the fact that $\mathbf{T}_C^{k+\tilde{t}} \Phi_V^{k+\tilde{t}} = \mathbf{T}_C^{k+\tilde{t}} \left[\Phi_V^{k:k+\tilde{t}} - \frac{1}{n} \mathbf{1}_V^{k+\tilde{t}} (\mathbf{v}^k)^\top \right] \mathbf{T}_C^k$ can be verified in the same way as in (28). (36) along with (35) implies the desired result (24).

A.3.3 Proof of (25)

Define a gradient matrix ∇^k in the same form as ∂^k , i.e.,

$$\begin{aligned}
\nabla^k &= [\nabla J^k; \mathbf{0}_{bn \times 2d}] \in \mathbb{R}^{\tilde{n} \times 2d}, \\
\nabla J^k &= [\nabla J_1^k; \dots; \nabla J_n^k] \in \mathbb{R}^{n \times 2d}, \\
\nabla J_i^k &= \nabla j_i(\mathbf{z}_i^k), \quad 1 \leq i \leq n.
\end{aligned} \tag{37}$$

By definition, $(\check{\mathbf{z}}_U^k)^\top = (\mathbf{u}^k)^\top \mathbf{Z}^k - (\mathbf{z}^*)^\top$. Repeating the first step in the above two proofs, we get

$$\begin{aligned}
(\mathbf{z}_U^{k+b})^\top &= (\mathbf{u}^{k+b})^\top \mathbf{Z}^{k+b} \\
&= (\mathbf{u}^{k+b})^\top \Phi_R^{k:k+b} \mathbf{Z}^{k+b} - \eta (\mathbf{u}^{k+b})^\top \sum_{t=0}^{b-1} \Phi_R^{k+t+1:k+b} \mathbf{I}_a^{k+t} \mathbf{V}^{k+t} \mathbf{Y}_V^{k+t} \\
&= (\mathbf{z}_U^k)^\top - \eta (\mathbf{u}^{k+b})^\top \sum_{t=0}^{b-1} \Phi_R^{k+t+1:k+b} \mathbf{I}_a^{k+t} \mathbf{V}^{k+t} \mathbf{Y}_V^{k+t}.
\end{aligned} \tag{38}$$

We extract the gradient of $J(\cdot)$ from (38) by defining

$$\begin{aligned}
(\mathbf{r}^{k,t})^\top &= \eta (\mathbf{u}^{k+b})^\top \Phi_R^{k+t+1:k+b} \mathbf{I}_a^{k+t} \mathbf{V}^{k+t}, \\
\eta^{k,t} &= (\mathbf{r}^{k,t})^\top \mathbf{1}_V^{k+t}, \quad \underline{\eta}^k = \sum_{t=0}^{b-1} \eta^{k,t}.
\end{aligned}$$

By $\nabla j(\mathbf{z}_U^k)$, the global gradient of \mathbf{z}_U^k , the last row in (38) is decomposed into

$$\begin{aligned}
(\mathbf{z}_U^{k+b} - \mathbf{z}^*)^\top &= (\mathbf{z}_U^k - \mathbf{z}^* - \underline{\eta}^k \nabla j(\mathbf{z}_U^k))^\top \\
&\quad + \sum_{t=0}^{b-1} \eta^{k,t} (\nabla j(\mathbf{z}_U^k)^\top - \mathbf{1}_n^\top \nabla^{k+t}) \\
&\quad - \sum_{t=0}^{b-1} (\mathbf{r}^{k,t})^\top (\mathbf{Y}_V^{k+t} - \mathbf{1}_V^{k+t} \mathbf{1}_n^\top \partial^{k+t}) \\
&\quad + \sum_{t=0}^{b-1} \eta^{k,t} [\mathbf{1}_n^\top (\nabla^{k+t} - \partial^{k+t})].
\end{aligned} \tag{39}$$

The first row of (39), $\mathbf{z}_U^k - \mathbf{z}^* - \underline{\eta}^k \nabla j(\mathbf{z}_U^k)$, depicts the gradient ascent/descent of the weight average variables \mathbf{z}_U^k , while the second to the fourth rows are bounded error terms, as proved in (40)-(42) below.

First, we have $\eta^{k,t} \leq \eta n$ and $\underline{\eta}^k \leq \eta bn$. Applying Lemma 2, we have $\|\mathbf{z}_U^k - \mathbf{z}^* - \underline{\eta}^k \nabla j(\mathbf{z}_U^k)\|_F \leq (1 - \eta \alpha bn) \|\mathbf{z}_U^k - \mathbf{z}^*\|_F$.

Second, let $\mathbf{1}_{n|\bar{n}} = [\mathbf{1}_n; \mathbf{0}_{\bar{n}-n}] \in \mathbb{R}^{\bar{n}}$, and $\mathbf{I}_{n|\bar{n}} = \text{diag}(\mathbf{1}_{n|\bar{n}}) \in \mathbb{R}^{\bar{n} \times \bar{n}}$. By direct computation, $\nabla j(\mathbf{z})^\top = \mathbf{1}_n^\top \nabla J(\mathbf{1}_n \mathbf{z}^\top)$, $\forall \mathbf{z}$. From (37), we obtain that for all k , $\mathbf{1}_{\bar{n}}^\top \nabla^k = \mathbf{1}_{n|\bar{n}}^\top \nabla^k = \mathbf{1}_n^\top \nabla J(\mathbf{Z}_0^k)$. Then,

$$\begin{aligned}
& \left\| \sum_{t=0}^{b-1} \eta^{k,t} (\nabla j(\mathbf{z}_U^k)^\top - \mathbf{1}_{\bar{n}}^\top \nabla^{k+t}) \right\|_F \\
&= \left\| \sum_{t=0}^{b-1} \frac{\eta^{k,t}}{n} (\mathbf{1}_n^\top \nabla J(\mathbf{1}_n (\mathbf{z}_U^k)^\top) - \mathbf{1}_n^\top \nabla J(\mathbf{Z}_0^{k+t})) \right\|_F \\
&\leq \eta \sqrt{n} \beta \sum_{t=0}^{b-1} \left\| \mathbf{1}_{n|\bar{n}}^\top (\mathbf{z}_U^k)^\top - \mathbf{1}_{n|\bar{n}}^\top \mathbf{u}^{k+t-1} \mathbf{Z}^{k+t} \right\|_F \\
&\leq 3\eta n \beta \sum_{t=0}^{b-1} \|\check{\mathbf{Z}}^{k+t}\|_F,
\end{aligned} \tag{40}$$

where the first inequality follows from (21). Third, it follows from (17) and (18) that

$$\begin{aligned}
& \left\| \sum_{t=0}^{b-1} (\mathbf{r}^{k,t})^\top (\mathbf{Y}_V^{k+t} - \mathbf{1}_V^{k+t} \mathbf{1}_{\bar{n}}^\top \partial^{k+t}) \right\|_F \\
&= \left\| \sum_{t=0}^{b-1} (\mathbf{r}^{k,t})^\top (\mathbf{Y}_V^{k+t} - \mathbf{1}_V^{k+t} (\mathbf{v}^{k+t})^\top \mathbf{Y}_V^{k+t}) \right\|_F \\
&\leq \sum_{t=0}^{b-1} \|\mathbf{r}^{k,t}\|_2 \|\check{\mathbf{Y}}_V^{k+t}\|_F \leq \eta n \sum_{t=0}^{b-1} \|\check{\mathbf{Y}}_V^{k+t}\|_F.
\end{aligned} \tag{41}$$

Moreover, similar to (35), we obtain,

$$\begin{aligned}
& \left\| \sum_{t=0}^{b-1} \eta^{k,t} [\mathbf{1}_{\bar{n}}^\top (\nabla^{k+t} - \partial^{k+t})] \right\|_F \\
&\leq \eta n \sum_{t=0}^{b-1} \left\| \sum_{i=1}^n \sum_{p=1}^{m_i} \nabla j_{i,p}(\mathbf{z}_i^k) - \nabla j_{i,p}(\mathbf{z}_i^k) \right\|_F \\
&\leq \eta n \beta \sum_{t=0}^{b-1} \sum_{j=t-bK+1}^t \|\mathbf{I}_{n|\bar{n}}(\mathbf{Z}^{t+1} - \mathbf{Z}^t)\|_F \\
&\leq \eta n \beta \sum_{t=0}^{b-1} \sum_{j=t-bK+1}^t (2\sqrt{n} \|\check{\mathbf{Z}}^j\|_F + \eta \|\mathbf{Y}^j\|_F).
\end{aligned} \tag{42}$$

Then, one can summarize (39)-(42) to get (25).

A.3.4 Proof of (26)

By (18) and (17), it holds that $\mathbf{1}_{\bar{n}}^\top \partial^k = (\mathbf{v}^{k+t})^\top \mathbf{Y}_V^k$ and

$$\begin{aligned}
\|\mathbf{Y}^k\|_F &= \|\mathbf{V}^k \mathbf{T}_C^k \mathbf{Y}_V^k + \frac{1}{n} \mathbf{V}^k (\mathbf{1}_V^k)^\top (\mathbf{v}^{k+t})^\top \mathbf{Y}_V^k\|_F \\
&\leq \|\mathbf{V}^k\|_2 \|\mathbf{T}_C^k \mathbf{Y}_V^k\|_F + \left\| \frac{1}{n} \mathbf{V}^k \mathbf{1}_V^k \mathbf{1}_{\bar{n}}^\top \partial^k \right\|_F \\
&\leq n \|\check{\mathbf{Y}}_V^k\|_F + \|\mathbf{1}_V^k \mathbf{1}_{\bar{n}}^\top \partial^k\|_F.
\end{aligned} \tag{43}$$

For the second term in (43), we have

$$\begin{aligned}
\|\mathbf{1}_V^k \mathbf{1}_n^T \partial^k\|_F &= \|\mathbf{1}_V^k (\mathbf{1}_n^T \partial J^k - \mathbf{1}_n^T \nabla J(\mathbf{1}_n(\mathbf{z}^*)^T))\|_F \\
&\leq \sqrt{\tilde{n}} \left\| \sum_{p=1}^{m_i} \sum_{i=1}^n (j_{i,p}(\mathbf{z}_i^{\tau_{i,p}^k}) - j_{i,p}(\mathbf{z}^*)) \right\| \\
&\leq \beta \sqrt{\tilde{n}} \sum_{t=k-bK}^{k-1} \|\mathbf{I}_{n|\tilde{n}} \mathbf{Z}^t - \mathbf{1}_{n|\tilde{n}}(\mathbf{z}^*)^T\|_F \\
&\leq \beta \sqrt{\tilde{n}} \sum_{t=k-bK}^k (2\sqrt{n} \|\check{\mathbf{Z}}^t\|_F + \sqrt{n} \|\mathbf{z}_U^t - \mathbf{z}^*\|_F)
\end{aligned} \tag{44}$$

Thus, we obtain (26) by using (43) and (44).

References

- [1] M. S. Assran and M. G. Rabbat. Asynchronous gradient push. *IEEE Transactions on Automatic Control*, 66(1):168–183, 2021.
- [2] Mahmoud Assran and Michael Rabbat. An empirical comparison of multi-agent optimization algorithms. In *IEEE Global Conference on Signal and Information Processing*, pages 573–577. IEEE, 2017.
- [3] Mahmoud Assran, Joshua Romoff, Nicolas Ballas, Joelle Pineau, and Mike Rabbat. Gossip-based actor-learner architectures for deep reinforcement learning. In *Advances in Neural Information Processing Systems*, pages 13299–13309, 2019.
- [4] Dimitri P Bertsekas and John N Tsitsiklis. *Parallel and distributed computation: numerical methods*. Athena Scientific, 1989.
- [5] Léon Bottou, Frank E Curtis, and Jorge Nocedal. Optimization methods for large-scale machine learning. *Siam Review*, 60(2):223–311, 2018.
- [6] Lucas Cassano, Kun Yuan, and Ali H Sayed. Multi-agent fully decentralized value function learning with linear convergence rates. *IEEE Transactions on Automatic Control*, 2020.
- [7] Tianyi Chen, Kaiqing Zhang, Georgios B Giannakis, and Tamer Başar. Communication-efficient distributed reinforcement learning. *arXiv preprint arXiv:1812.03239*, 2018.
- [8] Dongsheng Ding, Xiaohan Wei, Zhuoran Yang, Zhaoran Wang, and Mihailo R Jovanović. Fast multi-agent temporal-difference learning via homotopy stochastic primal-dual optimization. *arXiv preprint arXiv:1908.02805*, 2019.
- [9] Thinh Doan, Siva Maguluri, and Justin Romberg. Finite-time analysis of distributed TD(0) with linear function approximation on multi-agent reinforcement learning. In *International Conference on Machine Learning*, pages 1626–1635, 2019.
- [10] Simon S Du, Jianshu Chen, Lihong Li, Lin Xiao, and Dengyong Zhou. Stochastic variance reduction methods for policy evaluation. In *International Conference on Machine Learning*, pages 1049–1058, 2017.
- [11] Lasse Espeholt, Hubert Soyer, Remi Munos, Karen Simonyan, Vlad Mnih, Tom Ward, Yotam Doron, Vlad Firoiu, Tim Harley, Iain Dunning, Shane Legg, and Koray Kavukcuoglu. IMPALA: Scalable distributed deep-RL with importance weighted actor-learner architectures. In *International Conference on Machine Learning*, pages 1407–1416, 2018.

- [12] Hadrien Hendrikx, Francis Bach, and Laurent Massoulié. Asynchronous accelerated proximal stochastic gradient for strongly convex distributed finite sums. *arXiv preprint arXiv:1901.09865*, 2019.
- [13] Andreas VM Herz and Charles M Marcus. Distributed dynamics in neural networks. *Physical Review E*, 47(3):2155, 1993.
- [14] Haochen Jeff and Sra Suvrit. Random shuffling beats sgd after finite epochs. In *International Conference on Machine Learning*, pages 2624–2633. PMLR, 2019.
- [15] Soumya Kar, José MF Moura, and H Vincent Poor. Qd-learning: A collaborative distributed strategy for multi-agent reinforcement learning through consensus+innovations. *IEEE Transactions on Signal Processing*, 61:1848–1862, 2013.
- [16] Jens Kober, J Andrew Bagnell, and Jan Peters. Reinforcement learning in robotics: A survey. *The International Journal of Robotics Research*, 32(11):1238–1274, 2013.
- [17] Xiangru Lian, Wei Zhang, Ce Zhang, and Ji Liu. Asynchronous decentralized parallel stochastic gradient descent. In *International Conference on Machine Learning*, pages 3043–3052, 2018.
- [18] Patrick Mannion, Karl Mason, Sam Devlin, Jim Duggan, and Enda Howley. Dynamic economic emissions dispatch optimisation using multi-agent reinforcement learning. In *Proceedings of the Adaptive and Learning Agents Workshop (at AAMAS 2016)*, 2016.
- [19] Volodymyr Mnih, Adria Puigdomenech Badia, Mehdi Mirza, Alex Graves, Timothy Lillicrap, Tim Harley, David Silver, and Koray Kavukcuoglu. Asynchronous methods for deep reinforcement learning. In *International Conference on Machine Learning*, pages 1928–1937, 2016.
- [20] Volodymyr Mnih, Koray Kavukcuoglu, David Silver, Andrei A Rusu, Joel Veness, Marc G Bellemare, Alex Graves, Martin Riedmiller, Andreas K Fidjeland, Georg Ostrovski, et al. Human-level control through deep reinforcement learning. *Nature*, 518(7540):529–533, 2015.
- [21] Aryan Mokhtari and Alejandro Ribeiro. DSA: Decentralized double stochastic averaging gradient algorithm. *Journal of Machine Learning Research*, 17(61):1–35, 2016.
- [22] Angelia Nedic, Alex Olshevsky, and Wei Shi. Achieving geometric convergence for distributed optimization over time-varying graphs. *SIAM Journal on Optimization*, 27(4):2597–2633, 2017.
- [23] Angelia Nedić and Asuman Ozdaglar. Convergence rate for consensus with delays. *Journal of Global Optimization*, 47(3), 2010.
- [24] S. Pu, W. Shi, J. Xu, and A. Nedić. Push–pull gradient methods for distributed optimization in networks. *IEEE Transactions on Automatic Control*, 66(1):1–16, 2021.
- [25] Chao Qu, Shie Mannor, Huan Xu, Yuan Qi, Le Song, and Junwu Xiong. Value propagation for decentralized networked deep multi-agent reinforcement learning. In *Advances in Neural Information Processing Systems*, pages 1182–1191, 2019.
- [26] Guannan Qu, Yiheng Lin, Adam Wierman, and Na Li. Scalable multi-agent reinforcement learning for networked systems with average reward. *arXiv preprint arXiv:2006.06626*, 2020.
- [27] Muhammad I Qureshi, Ran Xin, Soumya Kar, and Usman A Khan. Push-saga: A decentralized stochastic algorithm with variance reduction over directed graphs. *arXiv preprint arXiv:2008.06082*, 2020.
- [28] Jineng Ren and Jarvis Haupt. A communication efficient hierarchical distributed optimization algorithm for multi-agent reinforcement learning. In *Real-world Sequential Decision Making Workshop at International Conference on Machine Learning*, 2019.

- [29] Mark Schmidt, Nicolas Le Roux, and Francis Bach. Minimizing finite sums with the stochastic average gradient. *Mathematical Programming*, 162(1-2):83–112, 2017.
- [30] David Silver, Julian Schrittwieser, Karen Simonyan, Ioannis Antonoglou, Aja Huang, Arthur Guez, Thomas Hubert, Lucas Baker, Matthew Lai, Adrian Bolton, et al. Mastering the game of go without human knowledge. *Nature*, 550(7676):354–359, 2017.
- [31] Richard S Sutton and Andrew G Barto. *Reinforcement learning: An introduction*. MIT press, 2018.
- [32] Richard S Sutton, Hamid Reza Maei, Doina Precup, Shalabh Bhatnagar, David Silver, Csaba Szepesvári, and Eric Wiewiora. Fast gradient-descent methods for temporal-difference learning with linear function approximation. In *Annual International Conference on Machine Learning*, pages 993–1000. ACM, 2009.
- [33] Y. Tian, Y. Sun, and G. Scutari. Achieving linear convergence in distributed asynchronous multiagent optimization. *IEEE Transactions on Automatic Control*, 65(12):5264–5279, 2020.
- [34] Behrouz Touri. *Product of random stochastic matrices and distributed averaging*. Springer Science & Business Media, 2012.
- [35] Elise Van der Pol and Frans A Oliehoek. Coordinated deep reinforcement learners for traffic light control. *Proceedings of Learning, Inference and Control of Multi-Agent Systems (at NIPS 2016)*, 2016.
- [36] Oriol Vinyals, Igor Babuschkin, Wojciech M Czarnecki, Michaël Mathieu, Andrew Dudzik, Junyoung Chung, David H Choi, Richard Powell, Timo Ewalds, Petko Georgiev, et al. Grandmaster level in starcraft ii using multi-agent reinforcement learning. *Nature*, 575(7782):350–354, 2019.
- [37] Hoi-To Wai, Zhuoran Yang, Princeton Zhaoran Wang, and Mingyi Hong. Multi-agent reinforcement learning via double averaging primal-dual optimization. In *Advances in Neural Information Processing Systems*, pages 9649–9660, 2018.
- [38] Pei Xie, Keyou You, Roberto Tempo, Shiji Song, and Cheng Wu. Distributed convex optimization with inequality constraints over time-varying unbalanced digraphs. *IEEE Transactions on Automatic Control*, 63(12):4331–4337, 2018.
- [39] R. Xin and U. A. Khan. A linear algorithm for optimization over directed graphs with geometric convergence. *IEEE Control Systems Letters*, 2(3):315–320, 2018.
- [40] R. Xin, S. Pu, A. Nedić, and U. A. Khan. A general framework for decentralized optimization with first-order methods. *Proceedings of the IEEE*, 108(11):1869–1889, 2020.
- [41] Ran Xin, Usman A Khan, and Soumya Kar. Variance-reduced decentralized stochastic optimization with accelerated convergence. *arXiv preprint arXiv:1912.04230*, 2019.
- [42] Jinming Xu, Shanying Zhu, Yeng Chai Soh, and Lihua Xie. Convergence of asynchronous distributed gradient methods over stochastic networks. *IEEE Transactions on Automatic Control*, 63(2):434–448, 2017.
- [43] K. Yuan, B. Ying, J. Liu, and A. H. Sayed. Variance-reduced stochastic learning by networked agents under random reshuffling. *IEEE Transactions on Signal Processing*, 67(2):351–366, 2019.
- [44] Jiaqi Zhang and Keyou You. Asynchronous decentralized optimization in directed networks. *arXiv preprint arXiv:1901.08215*, 2019.
- [45] Jiaqi Zhang and Keyou You. AsySPA: An exact asynchronous algorithm for convex optimization over digraphs. *IEEE Transactions on Automatic Control*, 2019.

- [46] Kaiqing Zhang, Zhuoran Yang, and Tamer Başar. Multi-agent reinforcement learning: A selective overview of theories and algorithms. *arXiv preprint arXiv:1911.10635*, 2019.
- [47] Kaiqing Zhang, Zhuoran Yang, Han Liu, Tong Zhang, and Tamer Başar. Fully decentralized multi-agent reinforcement learning with networked agents. In *International Conference on Machine Learning*, pages 5872–5881, 2018.